Mesenchymal stromal cells and alpha-1 antitrypsin have a strong synergy in modulating inflammation

Li Han[1,2], Xinran Wu[1], Ou Wang[3], William H. Velander[3], Michael Aynardi[4], E. Scott Halstead[5], Yulong Li[6], Yong Wang[1], Cheng Dong[1], and Yuguo Lei[1,2*]

1: Department of Biomedical Engineering, Pennsylvania State University, PA, USA

2: Huck Institutes of the Life Sciences, Pennsylvania State University, PA, USA

3: Department of Chemical and Biomolecular Engineering, University of Nebraska-Lincoln, NE, USA

4: Department of Orthopaedic Surgery, Pennsylvania State University College of Medicine, PA, USA

5: Division of Pediatric Critical Care Medicine, Department of Pediatrics, Pennsylvania State University College of Medicine, PA, USA

6: Department of Emergency Medicine, University of Nebraska Medical Center, NE, USA

* Corresponding Author

Yuguo Lei

The Pennsylvania State University, PA, USA

Email: yxl6034@psu.edu

Abstract:

Many reasons, such as infection, injury, tissue transplantation, and cancer treatment, can cause dysregulated hyperinflammation. Immune cells become excessive and hyperactive, producing sustained, systemic and large quantities of cytokines. The systemic inflammation can rapidly progress to disseminated intravascular coagulation, endothelium damage, capillary leakage, multiorgan (e.g., liver, kidney, heart, and brain) dysfunction, ARDS, and fatality. Although the initial driver may differ, the late-stage clinical features of hyperinflammation and cytokine storm converge. Unfortunately, the outcome of current treatments is still unsatisfactory. Our body has regulatory mechanisms to prevent the over-activation of immune cells, but these mechanisms fail or are insufficient in patients with hyperinflammation. Logically, augmenting these regulators represents a promising approach. Among the various natural negative regulators, mesenchymal stromal cells (MSCs) and alpha-1 antitrypsin (A1AT) are attractive due to their unique characteristics. MSCs and A1AT have shown capabilities to modulate immune cells. However, the efficacy and potency of MSCs or A1AT alone are limited and cannot fully normalize hyperinflammation and cytokine storm. Considering MSCs are cells while A1AT is a protein, we hypothesize that they may suppress inflammation using different mechanisms and have additive or synergistic effects when combined. This report showed that the combination of MSCs and A1AT was much more effective than individual components in modulating inflammation of various immune cells in vitro and in animal models. Our results provide solid evidence to support clinical studies of the combinational use of MSCs and A1AT for normalizing inflammation under various disease conditions.

Keywords: hyperinflammation, cytokine storm, mesenchymal stromal cells, alpha-1 antitrypsin, combination therapy

Introduction

Many reasons, such as infection, injury, transplantation, and cancer treatment, can cause inflammation[1–6]. An appropriate level of inflammation is needed to clean the pathogen and cell debris. Immune cells are expected to recognize the pathogens (or triggers), respond proportionally to the pathogen burden, and effectively eliminate the pathogens[7,8]. Subsequently, immune cells initiate the inflammation resolution program and return to homeostasis[9,10]. Cytokines are crucial in coordinating various immune cells to ensure a well-organized inflammation initiation, amplification, and resolution process with correct timing and amplitude. Cytokines guide the migration, proliferation, differentiation, and functions such as cytotoxicity, antigen presentation, and cytokine production of immune cells. Typically, cytokines have a short lifetime and stay at the injured sites to avoid systemic immune activation. Additionally, our body has negative regulators, including protein factors and cells, to further prevent systemic and hyperinflammation. For instance, natural receptors and cytokine antagonists such as IL-1 receptor antagonists can neutralize the off-target cytokines. There are also anti-inflammatory cytokines such as IL-10 and cells such as T_{reg} to prevent the overactivation of immune cells.

Under certain conditions, such as an overwhelming pathogen burden, inflammation becomes dysregulated, leading to hyperinflammation. For hyperinflammation, immune cells become excessive and hyperactive, producing sustained and large quantities of cytokines that cause elevated circulating levels, leading to systemic immune cell activation and cytokine production (i.e., cytokine storm)[1]. The systemic inflammation can rapidly progress to disseminated intravascular coagulation, endothelium damage, capillary leakage, multiorgan (e.g., liver, kidney, heart, and brain) dysfunction, ARDS, and fatality[11,12]. Although the initial driver may differ, the late-stage clinical features of hyperinflammation and cytokine storm converge.

The general strategy to treat hyperinflammation includes supportive care to maintain critical organ functions and to eliminate pathogens or triggers, such as using antibiotics. Additionally, various biologics (e.g., monoclonal antibodies) have been developed and used to neutralize cytokines or their receptors[1]. Small molecule drugs such as

glucocorticoids can also be used to suppress inflammation and the immune system. However, the treatment outcome is still unsatisfactory, with high fatality. In addition, there are significant limitations with current medications. First, neutralizing a particular cytokine elevated in a patient may not always be effective since other cytokines may play a critical role in the hyperinflammation circuit. Second, most of these therapeutics have significant side effects. Combining multiple therapeutics can lead to even higher side effects. Third, these treatments suppress normal immunity, making patients susceptible to secondary infections[1]. In short, safe therapeutics that can calm down the hyperactive immune cells while not impairing their immunity should be developed.

The human body has negative regulators, but these mechanisms fail or are insufficient in patients with hyperinflammation[9,10]. Logically, rejuvenating and augmenting these regulators represents a promising approach. Mesenchymal stromal cells (MSCs) are of particular interest among the various natural negative regulators due to their unique characteristics. MSCs are stromal cells that surveillance our tissue to maintain their homeostasis[13]. Upon injury or infection, MSCs can sense pathogen-associated molecular patterns (PAMPs) and damage-associated molecular patterns (DAMPs) and become pro-inflammatory cells, releasing proinflammatory cytokines to help initiate protective inflammation. However, when the cytokine level becomes high, cytokines will reprogram MSCs into an anti-inflammatory phenotype[13]. These primed MSCs use secreted molecules such as IDO and direct interaction to program monocytes and macrophages into the anti-inflammatory M2 phenotype[13–17]. And in turn, they program the adaptive immune cells into the anti-inflammatory phenotype, such as the T_{reg} cells. MSCs can also directly modulate the inflammation of T cells, B cells, NK cells, and neutrophils. Thus, MSCs act as a buffer system to ensure the inflammation of the injured site is in an appropriate range. MSCs are immunomodulators, not immunosuppressors[13].

In addition to their intelligence, MSCs have low immunogenicity. Therefore, Allogeneic MSCs can be administered without significant side effects. Many cases have shown that MSCs have excellent safety profiles in humans. Furthermore, MSCs can be isolated from various tissues, such as the placenta, umbilical cord, and adipose tissue. They can be efficiently expanded in vitro to produce cells at large scales. With these properties, MSCs

have been studied to modulate inflammation in various animal models such as GvHD, sepsis, and ARDS with positive outcomes[18–24]. In small clinical studies, MSCs have recently been used to treat severe COVID-19 patients, reducing the fatality significantly[25–27].

Alpha-1 antitrypsin (A1AT) is another negative regulator that is of high interest. A1AT is the second most abundant protein in plasma. It is an acute phase protein that increases its concentration up to 5-fold when the body is injured or infected. Recent research shows that A1AT has anti-inflammation, anti-protease, immunomodulation, cytoprotective, and pro-angiogenic activities[28,29,38,30–37]. It selectively inhibits neutrophil recruitment and cytokine production and neutralizes many proinflammatory cytokines[36,39–46]. It suppresses M1 macrophages while promoting M2 macrophages, T_{reg} cells, and tolerance dendritic cells s[28,47–54]. It also reduces bacterial and virus burden[55–63]. In addition, it protects cells from various stress[38,64–67] and promotes angiogenesis[68,69]. A1AT purified from plasma has been used to treat alpha-1 antitrypsin deficiency for decades with an excellent safety profile[70,71]. Typically, 4 g A1AT is infused each week intravenously to bring its concentration in plasma to 0.85 mg/mL. A1AT is being investigated in animal models for treating graft-versus-host disease[31,72,73], islet translation[74], heart attack[75], arthritis[76], liver failure[37], and diabetes[77,78].

In published results, MSCs and A1AT have shown capabilities in suppressing inflammation and modulating immune cells. However, the efficacy and potency of MSCs or A1AT alone are limited and cannot fully normalize hyperinflammation and cytokine storm. Considering MSCs are cells while A1AT is a protein, we hypothesize that they should suppress inflammation using different mechanisms and have additive or synergistic effects when combined. This report showed that the combination of MSCs and A1AT was much more effective than individual components in modulating the inflammation of various immune cells in vitro and animal models. Thus, the MSCs and A1AT combination has a high promise to treat inflammation and excessive cytokine production in various diseases.

Materials and Methods

MSC isolation

Full-term human placentas were obtained from Zenbio company. The procedure for isolating and expanding MSCs was similar to the published protocols with minor modifications[7]. Briefly, the placenta was washed and cut into 0.5 cm^3 pieces that were treated with TrypLE select solution (Gibco) at 37˚C for 30 min for partial digestion. When single cells were seen releasing from the tissues under a microscope, the partial digestion was stopped by adding the same volume of DMEM+10% FBS medium. The tissue was transferred into 50 mL tubes and settled for 3 min. After aspirating the supernatant, 15-20 partially digested pieces were plated in a 75 cm^2 tissue flask, and 9 mL of EBM-2 complete cell culture medium (EBM-2 +10% FBS+ 1% antibiotic) was added. The flasks were placed in an incubator without disturbing them for three days to allow tissues to adhere to the flask surface. After that, the culture medium was changed every three days until the cells reached 70% confluence. At that time, the remaining tissues were removed. Cells were dissociated with 2mL TrypLE selection solution per 75 cm^2 flask. These cells were considered passage 0 (P0). They were cryopreserved or subculture at a seeding density of 5,000 cells/cm^2 with EBM-2 CCM.

Surface marker verification

P4 MSCs were characterized with the Human Mesenchymal Stem Cell Verification Flow Kit (R&D Systems), including antibodies for positive markers CD90, CD73, CD105, and negative markers CD45, CD34, CD11b, CD79A, HLA-DR, as well as the Human Mesenchymal Stem Cells Multi-Color Flow Kit (R&D Systems) including antibodies for positive markers CD44, CD106, CD146, and CD166. 10 µL of each antibody was added to 100 µL cell suspension containing 1×10^5 MSCs and incubated at room temperature for 30 min, followed by wash and incubation with Goat Anti-Mouse IgG (H+L) Alexa Fluor 488 secondary antibody at room temperature in the dark for 30 min. Cells were analyzed with the BD FACSCanto™ II System.

MSC differentiation

Following the product instruction, the MSC differentiation capability was assessed using the Human Mesenchymal Stem Cell Functional Identification Kit (R&D System). The adipogenic differentiation medium and osteogenic differentiation medium were refreshed every three days. After 21 days, cells were fixed and stained with FABP-4 antibody to identify adipocytes or osteocalcin antibody to identify osteocytes.

IDO and PEG2 assay

P4 MSCs were stimulated with 10 ng/ml IFNγ and 15 ng/ml TNFα. Conditioned medium (CM) of the primed or unprimed MSCs was collected at 48 hours. The indoleamine 2,3-dioxygenase 1(IDO) expression level was measured with the IDO Activity Assay Kit (Abcam). The concentration of the Prostaglandin E2 (PGE2) was quantified with the Monoclonal Prostaglandin E2 ELISA Kit (Cayman Chemical).

Immune cell culture

Raw 264.7 cells (RAW-dual cells from InvivoGen) were cultured in the growth medium (DMEM, 4.5 g/l glucose, two mM L-glutamine, 10% heat-inactivated FBS, 100 µg/ml Normocin, 1% Pen-Strep) with an initial seeding density of 1.5×10^4 cells/cm^2. 200 µg/mL of Zeocin was added to maintain the selection pressure, and the medium was renewed twice a week. THP1 cells (THP1-dual cells from Invivo Gen) were maintained in the growth culture medium (RPMI 1640, 2 mM L-glutamine, 25 mM HEPES,10% heat-inactivated FBS, 100 µg/ml Normocin, and 1% Pen-Strep). In addition, 10 µg/ml of blasticidin and 100 µg/ml of Zeocin were added to maintain the selection pressure. HL-60 cells were maintained in Iscove's Modified Dulbecco's Medium (IMEM) with 20% FBS.

Macrophage inflammation assay

Raw 264.7 cells were stimulated with 100 ng/mL O111:B4 LPS (Sigma) and 10 ng/mL murine IFNγ (Peprotech). Human M0 macrophages were differentiated from THP1 monocytes by 24 h incubation with 100 ng/mL PMA(Sigma). Macrophages were then stimulated with 100 ng/mL O111:B4 LPS and 10 ng/mL human IFNγ. For treatment, A1AT was added to the medium. In addition, P4 MSCs were co-cultured with macrophages. Condition medium was harvested after 24 hours of incubation, and cytokines were

measured by ELISA.

Cytokine array

The quantitative levels of 40 mouse (for Raw 264.7 and BALF) or human (for PBMCs) cytokines in the conditioned medium with different treatments were evaluated with the Mouse or Human Inflammation Arrays (RyaBiotech) following their instructions. Briefly, the diluted condition medium and standards were incubated with the antibody array for 2 hours. Following washing, the array was incubated with Cy3 dye-labeled streptavidin. Array scanning and data extraction were done by RayBiotech using InnoScan 700/710 Microarray Scanner (Innopsys).

Neutrophil ROS and Netosis assays

The CellROX deep red reagent (Invitrogen) was used to measure intracellular ROS production. HL-60 cells were differentiated into neutrophil-like cells with 0.1 μM ATRA and 1.25% DMSO in RPMI1640 (with 10% FBS and 2mM L-Glutamine) for 3-5 days. Then cells were preloaded with 5 μM CellROX deep red reagent for 15 min at 37°C. After washing, cells were resuspended in fresh RPMI1640 complete medium and seeded into 96-well plates at 200,000 cells/mL. Cells were activated with either 100 nM PMA and treated with 0.5 mg/mL A1AT or 1/10 MSCs or their combination.

The Incucyte Cytotox Red Dye was applied to measure the Netosis. 100 μL of cells at 25,000 cells/mL were seeded in one well of a 96-well plate. Cells were immediately stimulated with PMA and treated with 0.5 mg/mL A1AT or 1/10 MSCs or their combination. The fluorescence and phase contrast images were taken by the FV3000 confocal laser scanning microscope (Olympus).

LPS-induced lung injury mice

O111:B4 LPS was dissolved in sterile phosphate-buffered saline (PBS). Pathogen-free 10 to 12 weeks old male C57BL/6 were purchased from Jackson Lab. The average body weight was about 25 g per mouse. All animal experiments were approved by the Animal Care and Use Committee of the University of Nebraska-Lincoln. For A1AT treatment, 2

mg A1AT in 200 μL PBS was injected intraperitoneally (IP) at 48 hr, 24 hr, and 0 hr before the LPS challenge (three doses). Before LPS instillation, mice were weighed and anesthesia by injecting ketamine (120 mg/kg body weight, BW) and xylazine (16 mg/kg BW) intraperitoneally. Mice were placed in the prone position. A 22 gauge (G) venous catheter was gently inserted into the trachea along the tongue's root in the vertical direction. Approximately 10 mm of the catheter was inserted. 50 μL of LPS was instilled via the catheter. For survival rate assay, 20 mg LPS/kg body weight was used. In addition, 10 mg LPS/kg body weight was used for lung tissue injury and cytokine assay. Using a pipette, 1×10^6 MSCs were injected in each mouse 30 min after the LPS challenge. 1 mL of air was added to the catheter to ensure the liquid volume was distributed well in the lung. The mouse's upper body was kept upright for 30 s to avoid fluid leakage. The body temperature was maintained at 37°C until full awareness. The mouse was transferred to ventilated cage individually with free access to food and water. The survival rate and body weight characteristics were monitored and recorded twice daily.

BALF and tissue harvest

Anesthesia was induced as described above. The trachea was carefully exposed with scissors and tweezers, and a 22 G venous catheter was inserted after a 5 mm cut to the trachea. 0.5 mL of sterile PBS was instilled, followed by 0.1 mL of air. After 60s, the fluid was aspirated. This process was repeated three times to collect all the bronchoalveolar lavage fluid (BALF). Cells in BALF were harvested by centrifuge of the BALF at 300 g for 10 min. BLAF cells were resuspended using 90%FBS with 10% DMSO and frozen in a Mr. Frost at -80°C before long-term storage in liquid nitrogen. After collecting BALF, the left and right lungs were removed and fixed in 4% PFA.

HE and immune staining

The fixed lung tissues were embedded in paraffin. 5 μm thick sections were cut (Epredia, Shando). The sections were dewaxed with the Leica Auto Stainer XL and then soaked with EDTA pH 8.0 (Abcam) or 10 mM Sodium Citrate solution pH 6.0 (Invitrogen) for antigen retrieval inside a domestic microwave oven. The superblock (TBS) blocking buffer was applied to the slide for 1 hr, followed by primary antibody incubation for 24 hrs

at 4 °C. Slides were washed with PBS and incubated with secondary antibody dilute and DAPI at room temperature in the dark. Slides were mounted with Shandon mount solution (Epredia Shandon).

BALF cells ICC staining

Cells collected from BALF were thawed and resuspended in PBS and then fixed in 4% PFA for 20 min. Next, cells were washed in dd H_2O, placed on a Poly-Prep Slide (Sigma), and heated until dry. Slides were blocked and stained as the tissue immune staining.

TUNEL staining

The paraffin sections from mice lung tissues were processed in the One-step TUNEL In Situ Apoptosis AF 594 Kit (Elabscience). Briefly, the sections were dewaxed by the Leica Auto Stainer XL and then treated with 1×proteinase K solution at 37°C for 20 mins. Then sections were labeled by TDT reaction mixture buffer for 2 hours at 37°C. Finally, the reaction was stopped by washing with PBS. The slide was stained with DAPI before mounting and signaling collection.

Results

Following published protocols, we isolated MSCs from the full-term placenta. Briefly, the placenta was cut into small pieces. Tissues were treated with TrypLE for 30 min and placed in cell culture flasks (Fig 1a). Cells migrated from the small tissue, adhered to the flask surface, and expanded. When cells reached about 70% confluence, the small tissues were removed, and cells were allowed to grow until full confluence (Fig 1b). These cells were then cryopreserved or subcultured (Fig 1c). Cells had the classical spindle-like morphology. Above 95% of the P4 cells expressed the classical MSC surface markers, including CD73, CD90, CD105, CD44, and CD166. The expression levels of the negative markers, including CD45, CD34, CD11b, CD79A, and HLA-DR, were neglectable (Fig 1d). In addition, MSCs could be differentiated into adipocytes and osteocytes. The day 21 product highly expressed the adipocyte marker FABP-4 and osteocyte marker

osteocalcin (Fig 1e). In summary, we successfully isolated MSCs from the placenta.

It is known that MSCs have anti-inflammation and immunomodulation capabilities. To test if our cells could suppress inflammation, we stimulated mouse Raw 264.7 macrophages (MΦs) with LPS and IFNγ to induce an intense inflammation. We optimized their concentrations and found 150 ng/mL LPS + 10 ng/mL IFNγ induced maximal cytokine release while not causing cell death. Inflamed cells were either untreated or treated with MSCs at three different dosages, i.e., 1 MSC for 1, 5, or 10 macrophages (1/1, 1/5, 1/10). Dexamethasone at 1 μg/mL, used in clinics to treat hyperinflammation, was used to benchmark MSC's capability. In addition, one sample was treated with MSC conditioned medium (CCM) to assess if the factors secreted by MSCs were effective. After 24 hrs treatment, the classical proinflammatory (IL-6 and TNF-α) and anti-inflammatory (IL-10) cytokines in the cell culture medium were measured with ELISA. The antibodies are specific to mouse proteins to avoid interference from the human cytokines secreted by MSCs. For IL6, all treatment groups reduced its expression (Fig 2a). Cells were better than dexamethasone when the cell dose was above 1/5. MSCs also decreased the TNFα secretion in a pattern similar to IL6 (Fig 2b).

All treatments increased the IL10 level. MSCs were better than dexamethasone and conditioned medium (Fig 2c). The ratios of IL6/IL10 or TNFα/IL10 can be used to assess the inflammation/an-inflammation balance. Our data showed that dexamethasone decreased the IL6/IL10 from 8 to 3.5, and MSCs decreased the IL6/IL10 to 1.5 for 1/10 dosage and to <0.5 for 1/5 and 1/1 dosages. Conditioned medium reduced the ratio to 1.5 (Fig 2d). Dexamethasone decreased the TNFα/IL10 from 38 to 18. MSCs decreased the TNFα/IL10 to ~5, while the conditioned medium reduced the ratio to ~10 (Fig 2e). The results showed that i) MSCs could inhibit the proinflammatory cytokine secretion while promoting the anti-inflammatory cytokine secretion from Raw 264.7 macrophages; ii) cells were better than their conditioned medium and dexamethasone; iii) there was no huge difference between the 1/10, 1/5 and 1/1 dose for MSCs in terms of the IL6/IL10 or TNFα/IL10 ratios. Thus, we decided to use MSCs at 1/10 dose for the rest of this paper.

We evaluated A1AT's capability to suppress inflammation in Raw 264.7 macrophages.

Similar to the first experiment, macrophages were stimulated with LPS and IFNγ to induce inflammation. Inflame cells were either untreated or treated with A1AT (isolated from human plasma) with concentrations ranging from 0.1 to 2.0 mg/mL. Dexamethasone at 1 μg/mL was done to benchmark A1AT's capability. After 24 hrs treatment, the classical proinflammatory (IL6 and TNFα) and anti-inflammatory (IL10) cytokines in the cell culture medium were measured with ELISA. We found that A1AT reduced the IL6 and TNFα levels at all tested concentrations. The IL6 level was inversely proportional to the A1AT concentration (Fig 3a, b). A1AT at a concentration ≥0.5mg/mL significantly increased IL10 expression (Fig 3c). Dexamethasone stimulated much less IL10 expression. Dexamethasone decreased the IL6/IL10 from 7.5 to 2.2 (Fig 3d). A1AT decreased the IL6/IL10 to <0.5 when ≥0.5 mg/mL protein was used. Dexamethasone decreased the TNFα/IL10 from 30 to 15 (Fig 3e). A1AT decreased the TNFα/IL10 to ~2 when the protein was ≥0.5 mg/mL. The results showed that i) A1AT could inhibit the proinflammatory cytokine secretion while promoting the anti-inflammatory cytokine secretion from Raw 264.7 cells; ii) there was no huge difference between the 0.5, 1.0, and 2.0 mg/mL A1AT in terms of the IL6/IL10 or TNFα/IL10 ratios. Thus, we decided to use 0.5 mg/mL A1AT for the rest of this paper.

Next, we studied if MSCs and A1AT had synergistic effects on suppressing inflammation. We treated inflamed Raw 264.7 macrophages with 0.5 mg/mL A1AT, or 1/10 MSCs, or their combination. We showed that all the treatments reduced the IL6 and TNFα levels while increasing the IL10 level, with the MSCs+A1AT combination having the most potent effect (Fig 4a-c). This is obvious when looking at the IL6/IL10 or TNFα/IL10 ratios (Fig 4d-e). The results show that MSCs and A1AT synergistically suppress mouse macrophage inflammation.

Inflamed cells secreted many cytokines. We quantitively measured 40 inflammation-related cytokines using an antibody array. The identities and functions of these cytokines are summarized in Table S1. The treatments affected the expression of 19 cytokines. A1AT reduced the expression of CCL17, CCL2 (MCP-1), CCL5 (RANTES), CXCL1, CXCL9, IFNγ, IL-13, IL-15, IL-1a and IL-6 (Table S2). MSCs reduced the expression of CCL17, CCL2, CXCL9, GM-CSF, IFNγ, IL-13, IL-15, IL-1a, IL-1b, IL-6 and TNFα. A1AT

and MSCs showed a strong synergy in regulating the expression of CCL17, CCL5, CXCL1, CXCL13, CXCL9, G-CSF, GM-CSF, IFNγ, IL-10, IL-13, IL-15, IL-17, IL-1a, IL-1b, IL-2, IL-6, IL-7, and TNFα.

We categorized these cytokines into several categories (Table S3) based on their response pattern to the treatments. For Category A proinflammatory cytokines (CCL17, CXCL9, IFNγ, IL13, IL15, IL1a, IL6), MSCs and A1AT reduced their expressions, and MSCs and A1AT showed a strong synergistic effect. For Category B proinflammatory cytokines (CCL5, CXCL1), A1AT but not MSCs reduced their expressions. However, MSCs boosted A1AT's effect. For Category C proinflammatory cytokines (GM-CSF, IL-1b, TNFa), MSCs but not A1AT reduced their expressions. However, A1AT boosted MSCs' effect. For Category D proinflammatory cytokines (CXCL13, G-CSF, IL7), MSCs or A1AT alone had no effects, but their combination reduced the cytokine expression significantly. For Category E proinflammatory cytokines (IL2), only A1AT had no effect, and MSCs did not affect A1AT's capability. For Category F proinflammatory cytokines (IL17), only MSCs had no effect, and A1AT did not affect MSCs' capability. For Category G proinflammatory cytokines (CCL2), both A1AT and MSCs had an effect, but they had no synergy. Category H is ant-inflammatory cytokines; both A1AT and MSCs showed effects and had a strong synergy. In summary, the results show i) the cytokines affected by A1AT and MSCs were not identical, indicating they used different mechanisms of action, and ii) MSCs and A1AT have synergistic effects on regulating the expression of many cytokines.

The above studies used mouse macrophages. We then tested if MSCs and A1AT could suppress the inflammation in human macrophages. THP-1 monocytes were first differentiated into macrophages. Inflammation was then induced using LPS and IFNγ. Treatments were also added. The results from human macrophages (Fig 6) were similar to those from Raw 264.7 macrophages (Fig 4). All the treatments reduced IL6 and TNFα levels while increasing IL10. The MSC and A1AT combination was much more effective than the individual components. The results show that the capabilities of MSCs and A1AT and their synergistic effects on suppressing macrophage inflammation are cross-species.

We then used primary PBMCs to confirm the anti-inflammation capabilities of MSCs and A1AT. To avoid donor-to-donor variations, we used PBMCs pooled from multiple donors. We added LPS and IFNγ to activate the innate cells and anti-CD3 and anti-CD28 antibodies to activate T cells. We found that all treatments reduced the IL6 and TNFα secretion while increasing the IL10 production. Again, MSC and A1AT combination was much more effective than the individual components (Fig 7).

During hyperinflammation, neutrophils were activated, generating large amounts of reactive oxidative species (ROS) and neutrophil extracellular traps (NETs). While ROS and NETs can help eliminate pathogens, they also exaggerate cytokine storms, damage tissue barriers, and cause intravascular coagulation and multiple organ dysfunction. Literature research finds that both MSCs and A1AT can inhibit ROS and NETs production. We thus tested if they had synergy. HL-60 cells were differentiated into neutrophils that were then activated with PMAs. PI dye staining showed that MSCs and A1AT could reduce neutrophil death, and their combination worked better to protect neutrophils (Fig 8a, b). During hyperinflammation, extensive neutrophil death release DAMPs, ROS, and toxic chemicals that exaggerate hyperinflation and cause tissue damage. Reducing neutrophil death can reduce the release of toxic chemicals from dead cells. MSC and A1AT showed a significant synergy to reduce the production of ROS (Fig 8c, d) and NETs (Fig 8e, f). We also measured the cytokine levels in the medium. All the treatments reduced IL6 and TNFα levels while increasing IL10. The MSC and A1AT combination worked better than the individual components (Fig 9). In summary, MSCs and A1AT have a substantial synergy to modulate the inflammation, ROS production, NETosis, and death of neutrophils.

NF-κB and IRF are critical pathways for inflammation. To evaluate if the treatments regulate these pathways, Raw 264.7 and THP1 cells were engineered to express a SEAP reporter for the NF-κB pathway and a luciferase reporter for the IRF pathway. THP-1 cells were differentiated into macrophages, as described previously. We found that MSCs and A1AT inhibited both pathways of the two cell types and showed strong synergistic effects (Fig 10).

We then used the LPS-induced acute lung injury model to test if our in vitro results could be replicated in vivo. A lethal dosage (20 mg LPS/kg body weight) was administrated to the first cohort of mice to test the capabilities of treatments to reduce mortality. All mice died in 3 days without treatment. MSCs or A1AT alone increased the survival rate. The combination treatment completely protected mice from death (Fig 11b). The body weight measurements agreed with the mortality. The combination treatment had significantly less body weight reduction (Fig 11c).

A high but non-lethal dosage (10 mg LPS/kg body weight) was administrated to the second cohort of mice to test if treatments could modulate the hyperinflammation and reduce tissue injuries. First, we analyzed lung tissue injuries via H&E staining. Images were analyzed by trained pathologists blindly, and scored based on five criteria, including i) the number of neutrophils in alveolar space; ii) the number of neutrophils in interstitial space; iii) the amount of hyaline membranes; iv) the amount of proteinaceous debris filling the airspaces, and v) the alveolar septal thickening. We found that MSC and A1AT reduced the overall lung injury, while their combo worked significantly better (Fig 12).

We harvested the bronchoalveolar lavage fluid (BALF) for protein and immune cell analyses. A high total protein concentration indicates the disruption of the endothelium and epithelium integrity. MSCs or A1AT alone could significantly reduce the total protein level, and their combination worked significantly better (Fig 13a), showing their capability to protect endothelium and epithelium. Similar to the in vitro assays, MSCs and A1AT reduced the IL6 and TNFα while increasing the IL10 level significantly. Their combination was much more effective than individual components (Fig 13b-f). We used the Raybiotech Inflammation Antibody Array to quantitively measure 40 inflammation-related cytokines (Fig 14, Table S2). The treatments affected the expression of 19 cytokines. A1AT reduced the expression of CCL3, CXCL1, CXCL13, CXCL9, IFNγ, IL-12p70, IL-1b, IL-2, IL-5, IL-6, IL-7, Leptin and TNFα, while increasing the IL-4 level (Table S3). MSCs reduced the expression of CCL3, CXCL1, CXCL9, IFNγ, IL-12p70, IL-15, IL-17, IL-1b, IL-3, IL-5, IL-6, IL-7, Leptin and TNFα. A1AT and MSCs showed a strong synergy in regulating the expression of CCL5 (RANTES), CXCL1, CXCL9, IFNγ, IL-10, IL-12p70, IL-15, IL-17, IL-1a, IL-1b, IL-2, IL-3, IL-4, IL-5, IL-6, IL-7, Leptin and TNFα.

We analyzed the immune cells in BALF. We found that MSCs, A1AT, and especially their combination, reduced the number of total cells, macrophages, and neutrophils in BALF. The MSC and A1AT combination functioned better than the individual components (Fig 15). We used the TUNNEL staining to identify dead cells in the lung tissues. Both MSCs and A1AT reduced the number of dead cells. Astonishingly, almost no dead cells could be found in the combination treatment group (Fig 16).

Conclusions

In this project, we showed that MSCs and A1AT had a strong synergy in 1) suppressing the cytokine releases from various immune cells, including macrophages, neutrophils, and PBMCs under inflammation conditions; 2) reducing cell death, ROS production, and NETosis in neutrophils; and 3) inhibiting NF-κB and IRF pathways in vitro; and 4) reduced the cytokine production, immune cell infiltration, lung tissue damages and mortalities in mouse ALI model. The in vitro and in vivo data agreed well. Both MSCs and A1AT have been used in clinics with excellent safety profiles. Our results provide solid evidence to support clinical studies of the combinational use of MSCs and A1AT for normalizing inflammation under various disease conditions.

References:

1. Fajgenbaum, D. C. & June, C. H. Cytokine Storm. *N. Engl. J. Med.* **383**, 2255–2273 (2020).

2. Hussen, J., Kandeel, M., Hemida, M. G. & Al-Mubarak, A. I. A. Antibody-based immunotherapeutic strategies for COVID-19. *Pathogens* **9**, 1–18 (2020).

3. Kiselevskiy, M. *et al.* Immune pathogenesis of covid-19 intoxication: Storm or silence? *Pharmaceuticals* **13**, 1–17 (2020).

4. Nouveau, L. *et al.* Immunological analysis of the murine anti-CD3-induced cytokine release syndrome model and therapeutic efficacy of anti-cytokine antibodies. *Eur. J. Immunol.* **51**, 2074–2085 (2021).

5. Kash, J. C. *et al.* Genomic analysis of increased host immune and cell death responses induced by 1918 influenza virus. *Nature* **443**, 578–581 (2006).

6. Morgan, R. A. *et al.* Case report of a serious adverse event following the administration of t cells transduced with a chimeric antigen receptor recognizing ERBB2. *Mol. Ther.* **18**, 843–851 (2010).

7. A current view on inflammation. *Nat. Immunol.* **18**, 825 (2017).

8. Netea, M. G. *et al.* A guiding map for inflammation. *Nat. Immunol.* **18**, 826–831 (2017).

9. Fullerton, J. N. & Gilroy, D. W. Resolution of inflammation: A new therapeutic frontier. *Nat. Rev. Drug Discov.* **15**, 551–567 (2016).

10. Feehan, K. T. & Gilroy, D. W. Is Resolution the End of Inflammation? *Trends Mol. Med.* **25**, 198–214 (2019).

11. Mahmudpour, M., Roozbeh, J., Keshavarz, M., Farrokhi, S. & Nabipour, I. COVID-19 cytokine storm: The anger of inflammation. *Cytokine* **133**, 155151 (2020).

12. Ghanbarpour, R. *et al.* Pulmonary infections in ICU patients without underlying disease on ventilators. *Trauma Mon.* **19**, 41–44 (2014).

13. Bernardo, M. E. & Fibbe, W. E. Mesenchymal stromal cells: Sensors and switchers of inflammation. *Cell Stem Cell* **13**, 392–402 (2013).

14. Kyurkchiev, D. Secretion of immunoregulatory cytokines by mesenchymal stem cells. *World J. Stem Cells* **6**, 552 (2014).

15. Park, C. W. *et al.* Cytokine secretion profiling of human mesenchymal stem cells by antibody array. *Int. J. stem cells* **2**, 59–68 (2009).

16. Metcalfe, S. M. Mesenchymal stem cells and management of COVID-19 pneumonia. *Med. Drug Discov.* **5**, 100019 (2020).

17. Liang, X., Ding, Y., Zhang, Y., Tse, H. F. & Lian, Q. Paracrine mechanisms of mesenchymal stem cell-based therapy: Current status and perspectives. *Cell Transplant.* **23**, 1045–1059 (2014).

18. Kim, M. *et al.* Soluble PTX3 of Human Umbilical Cord Blood-Derived Mesenchymal Stem Cells Attenuates Hyperoxic Lung Injury by Activating Macrophage Polarization in Neonatal Rat Model. *Stem Cells Int.* **2020**, (2020).

19. Le Blanc, K. *et al.* Mesenchymal stem cells for treatment of steroid-resistant, severe, acute graft-versus-host disease: a phase II study. *Lancet* **371**, 1579–1586 (2008).

20. Qu, G. *et al.* Immunomodulatory function of mesenchymal stem cells: regulation and application. *J. Cell. Immunother.* **4**, 1–3 (2018).

21. Karussis, D. *et al.* Safety and immunological effects of mesenchymal stem cell transplantation in patients with multiple sclerosis and amyotrophic lateral sclerosis. *Arch. Neurol.* **67**, 1187–1194 (2010).

22. Connick, P. *et al.* Autologous mesenchymal stem cells for the treatment of secondary progressive multiple sclerosis: An open-label phase 2a proof-of-concept study. *Lancet Neurol.* **11**, 150–156 (2012).

23. Lombardo, E. Mesenchymal stem cells as a therapeutic tool to treat sepsis. *World J. Stem Cells* **7**, 368 (2015).

24. Wilson, J. G. *et al.* Mesenchymal stem (stromal) cells for treatment of ARDS: A phase 1 clinical trial. *Lancet Respir. Med.* **3**, 24–32 (2015).

25. Liang, B. *et al.* Clinical remission of a critically ill COVID-19 patient treated by human umbilical cord mesenchymal stem cells. *ChinaXiv* (2020) doi:10.3969/j.issn.2095-4344.2012.49.011.

26. Leng, Z. *et al.* Transplantation of ACE2- Mesenchymal stem cells improves the outcome of patients with covid-19 pneumonia. *Aging Dis.* **11**, 216–228 (2020).

27. Lanzoni, G. *et al.* Umbilical cord mesenchymal stem cells for COVID-19 acute respiratory distress syndrome: A double-blind, phase 1/2a, randomized controlled trial. *Stem Cells Transl. Med.* **10**, 660–673 (2021).

28. Guttman, O., S Freixo-Lima, G. & C Lewis, E. Alpha1-antitrypsin, an endogenous immunoregulatory molecule: distinction between local and systemic effects on tumor immunology. *Integr. Cancer Sci. Ther.* **2**, 272–280 (2016).

29. Bergin, D. A., Hurley, K., McElvaney, N. G. & Reeves, E. P. Alpha-1 antitrypsin: A potent anti-inflammatory and potential novel therapeutic agent. *Arch. Immunol. Ther. Exp. (Warsz).* **60**, 81–97 (2012).

30. Janciauskiene, S. *et al.* The Multifaceted Effects of Alpha1-Antitrypsin on Neutrophil Functions. *Front Pharmacol.* **17**, 341 (2018).

31. Marcondes, A. M. *et al.* Inhibition of IL-32 activation by α-1 antitrypsin suppresses alloreactivity and increases survival in an allogeneic murine marrow transplantation model. *Blood.* **118**, 5031–9 (2011).

32. Shapiro, S. D. *et al.* Neutrophil Elastase Contributes to Cigarette Smoke-Induced Emphysema in Mice. *Am. J. Pathol.* **163**, 2329–2335 (2003).

33. Kidokoro Y, Kravis TC, Moser KM, Taylor JC, C. I. Relationship of Leukocyte Elastase Concentration to Severity of Emphysema in Homozygous α1-Antitrypsin-

Deficient Persons. *Am Rev Respir Dis.* **115**, 793–803 (1977).

34. Yuan-Ping Han, Chunli Yan, and W. L. G. Proteolytic Activation of Matrix Metalloproteinase-9 in Skin Wound Healing Is Inhibited by α-1-Antichymotrypsin. *J Invest Dermatol.* **128**, 2334–2342 (2008).

35. He, S., Chen, H. & Zheng, J. Inhibition of tryptase and chymase induced nucleated cell infiltration by proteinase inhibitors 1. *Acta Pharmacol Sin.* **25**, 1677–1684 (2004).

36. Bergin, D. A. *et al.* α-1 antitrypsin regulates human neutrophil chemotaxis induced by soluble immune complexes and IL-8. *J. Clin. Invest.* **120**, 4236–4250 (2010).

37. Jedicke, N. *et al.* α-1-antitrypsin inhibits acute liver failure in mice. *Hepatology.* **59**, 2299–2308 (2014).

38. Toldo, S. *et al.* Alpha-1 antitrypsin inhibits caspase-1 and protects from acute myocardial ischemia-reperfusion injury. *J. Mol. Cell. Cardiol.* **51**, 244–251 (2011).

39. Libert, C., Molle, W. Van, Brouckaert, P. & Fiers, W. Alpha-1-Antitrypsin Inhibits the Lethal Response to TNF in Mice. *J. Immunol.* **157**, 5126–5129 (1996).

40. Subramaniyam, D. *et al.* Effects of alpha 1-antitrypsin on endotoxin-induced lung inflammation in vivo. *Inflamm. Res.* **59**, 571–578 (2010).

41. Griese, M. *et al.* α1-Antitrypsin inhalation reduces airway inflammation in cystic fibrosis patients. *Eur. Respir. J.* **29**, 240–250 (2007).

42. Pott, G. B., Chan, E. D., Dinarello, C. A. & Shapiro, L. α-1-Antitrypsin is an endogenous inhibitor of proinflammatory cytokine production in whole blood. *J. Leukoc. Biol.* **85**, 886–895 (2009).

43. Ochayon, D. E., Mizrahi, M., Shahaf, G., Baranovski, B. M. & Lewis, E. C. Human α1-Antitrypsin Binds to Heat-Shock Protein gp96 and Protects from Endogenous gp96-Mediated Injury In vivo. *Front. Immunol.* **4**, 320 (2013).

44. Tilg, B. H., Vannier, E., Vachino, G., Dinardlo, C. A. & Mier, J. W. Antiinflammatory properties of hepatic acute phase proteins: preferential induction of interleukin 1 (IL-1) receptor antagonist over IL-1 beta synthesis by human peripheral blood mononuclear cells. *J Exp Med.* **178**, 1629–36 (1993).

45. Finotti, P. & Pagetta, A. A heat shock protein70 fusion protein with alpha1-antitrypsin in plasma of type 1 diabetic subjects. *Biochem Biophys Res Commun.* **315**, 297–305 (2004).

46. Lockett, A. D. *et al.* α_1-Antitrypsin modulates lung endothelial cell inflammatory responses to TNF-α. *Am J Respir Cell Mol Biol.* **49**, 143–50 (2013).

47. Chan, E. D. *et al.* Alpha-1-antitrypsin inhibits nitric oxide production. *J. Leukoc. Biol.* **92**, 1251–1260 (2012).

48. Zhou, T. *et al.* Alpha-1 antitrypsin attenuates M1 microglia-mediated neuroinflammation in retinal degeneration. *Front. Immunol.* **9**, 1202 (2018).

49. Jonigk, D. *et al.* Anti-inflammatory and immunomodulatory properties of 1-antitrypsin without inhibition of elastase. *Proc. Natl. Acad. Sci.* **110**, 15007–15012 (2013).

50. Serban, K. A. *et al.* Alpha-1 antitrypsin supplementation improves alveolar macrophages efferocytosis and phagocytosis following cigarette smoke exposure. *PLoS One* **12**, 1–17 (2017).

51. Nita, I. M., Serapinas, D. & Janciauskiene, S. M. α1-Antitrypsin regulates CD14 expression and soluble CD14 levels in human monocytes in vitro. *Int. J. Biochem. Cell Biol.* **39**, 1165–1176 (2007).

52. Janciauskiene, S. M., Nita, I. M. & Stevens, T. α1-antitrypsin, old dog, new tricks: α1- antitrypsin exerts in vitro anti-inflammatory activity in human monocytes by elevating cAMP. *J. Biol. Chem.* **282**, 8573–8582 (2007).

53. Ozeri, E., Mizrahi, M., Shahaf, G. & Lewis, E. C. -1 Antitrypsin Promotes Semimature, IL-10-Producing and Readily Migrating Tolerogenic Dendritic Cells. *J. Immunol.* **189**, 146–153 (2012).

54. Churg, A. *et al.* Alpha-1-Antitrypsin and a Broad Spectrum Acute Anti-Inflammatory Effects. *Lab Invest* **81**, 1119–1131 (2001).

55. Kaner, Z. *et al.* Acute Phase Protein α1-Antitrypsin Reduces the Bacterial Burden in Mice by Selective Modulation of Innate Cell Responses. *J. Infect. Dis.* **211**, 1489–1498 (2015).

56. Pott, G. B., Beard, K. S., Bryan, C. L., Merrick, D. T. & Shapiro, L. Alpha-1 Antitrypsin Reduces Severity of Pseudomonas Pneumonia in Mice and Inhibits Epithelial Barrier Disruption and Pseudomonas Invasion of Respiratory Epithelial Cells. *Front. Public Heal.* **1**, 1–13 (2013).

57. Wanner, A., Arce, A. De & Pardee, E. Novel therapeutic uses of alpha-1 antitrypsin: A window to the future. *COPD J. Chronic Obstr. Pulm. Dis.* **9**, 583–588 (2012).

58. Jia, Q. *et al.* Short cyclic peptides derived from the C-terminal sequence of α1-antitrypsin exhibit significant anti-HIV-1 activity. *Bioorganic Med. Chem. Lett.* **22**, 2393–2395 (2012).

59. Bristow CL, Modarresi R, Babayeva MA, LaBrunda M, Mukhtarzad R, Trucy M, Franklin A, Reeves RE, Long A, Mullen MP, Cortes J, W. R. A feedback

regulatory pathway between LDL and alpha-1 proteinase inhibitor in chronic inflammation and infection. *Discov Med.* **16**, 201–18 (2013).

60. Bristow, C. L., Babayeva, M. A., LaBrunda, M., Mullen, M. P. & Winston, R. α 1proteinase inhibitor regulates CD4 + lymphocyte levels and is rate limiting in HIV-1 disease. *PLoS One* **7**, 1–10 (2012).

61. Abdulsalam, S. I., Abdulatif, A., Joyal, J., Wisam, G. & Ajayeb, A. Increased Prevalence of the Alpha-1-Antitrypsin (A1AT) Deficiency-Related S Gene in Patients Infected With Human Immunodeficiency Virus Type 1. *J. Med. Virol.* **81**, 1047–1051 (2009).

62. Münch, J. *et al.* Discovery and Optimization of a Natural HIV-1 Entry Inhibitor Targeting the gp41 Fusion Peptide. *Cell* **129**, 263–275 (2007).

63. SHAPIRO, L., POTT, G. B. & RALSTON, A. H. Alpha-1-antitrypsin inhibits human immunodeficiency virus type 1. *FASEB J.* **15**, 115–122 (2002).

64. Moldthan, H. L. *et al.* Alpha 1-antitrypsin therapy mitigated ischemic stroke damage in rats. *J. Stroke Cerebrovasc. Dis.* **23**, e355–e363 (2014).

65. Koulmanda, M. *et al.* Alpha 1-antitrypsin reduces inflammation and enhances mouse pancreatic islet transplant survival. *Proc. Natl. Acad. Sci.* **109**, 15443–15448 (2012).

66. Petrache, I. *et al.* Alpha-1 Antitrypsin Inhibits Antitrypsin Inhibits Caspase-3 Activity , Preventing Lung Endothelial Cell Apoptosis. *Am. J. Pathol.* **169**, 1155–1166 (2006).

67. Kalis, M., Kumar, R., Janciauskiene, S., Salehi, A. & Cilio, C. M. A 1-Antitrypsin Enhances Insulin Secretion and Prevents Cytokine-Mediated Apoptosis in Pancreatic B-Cells. *Islets* **2**, 185–189 (2010).

68. Bellacen, K., Kalay, N., Ozeri, E., Shahaf, G. & Lewis, E. C. Revascularization of pancreatic islet allografts is enhanced by α-1-Antitrypsin under anti-inflammatory conditions. *Cell Transplant.* **22**, 2119–2133 (2013).

69. Aldonyte, R. *et al.* Endothelial alpha-1-antitrypsin attenuates cigarette smoke induced apoptosis in vitro. *COPD J. Chronic Obstr. Pulm. Dis.* **5**, 153–162 (2008).

70. Janciauskiene, S. & Welte, T. Well-known and less well-known functions of Alpha-1 antitrypsin: Its role in chronic obstructive pulmonary disease and other disease developments. *Ann. Am. Thorac. Soc.* **13**, S280--S288 (2016).

71. Kim, M., Cai, Q. & Oh, Y. Therapeutic potential of alpha-1 antitrypsin in human disease. *Ann. Pediatr. Endocrinol. Metab.* **23**, 131–135 (2018).

72. Marcondes, A. M. *et al.* α-1-Antitrypsin (AAT)-modified donor cells suppress

GVHD but enhance the GVL effect: a role for mitochondrial bioenergetics. *Blood.* **124**, 2881–2892 (2014).

73. Tawara, I. *et al.* Alpha-1-antitrypsin monotherapy reduces graft-versus-host disease after experimental allogeneic bone marrow transplantation. *Proc Natl Acad Sci USA* **109**, 564 (2012).

74. Song, S., Goudy, K., Wasserfall, C., Wang, J. & Tang, Q. Recombinant adeno-associated virus-mediated alpha-1 antitrypsin gene therapy prevents type I diabetes in NOD mice. *Gene Ther.* **11**, 181–186 (2004).

75. Toldo, S. *et al.* antitrypsin inhibits caspase-1 and protects from acute myocardial ischemia – reperfusion injury. *J. Mol. Cell. Cardiol.* **51**, 244–251 (2011).

76. Grimstein, C. *et al.* Alpha-1 antitrypsin protein and gene therapies decrease autoimmunity and delay arthritis development in mouse model. *J Transl Med.* **24**, 21 (2011).

77. Ma, H., Lu, Y. & Li, H. Intradermal α 1-antitrypsin therapy avoids fatal anaphylaxis , prevents type 1 diabetes and reverses hyperglycaemia in the NOD mouse model of the disease. *Diabetologia* **53**, 2198–2204 (2010).

78. Guttman, O., Yossef, R., Freixo-lima, G., Porgador, A. & Lewis, E. C. a1-Antitrypsin modifies general natural killer cell interactions with dendritic cells and specific interactions with islet b -cells in favour of protection from autoimmune diabetes. *Immunology.* 530–539 (2014).

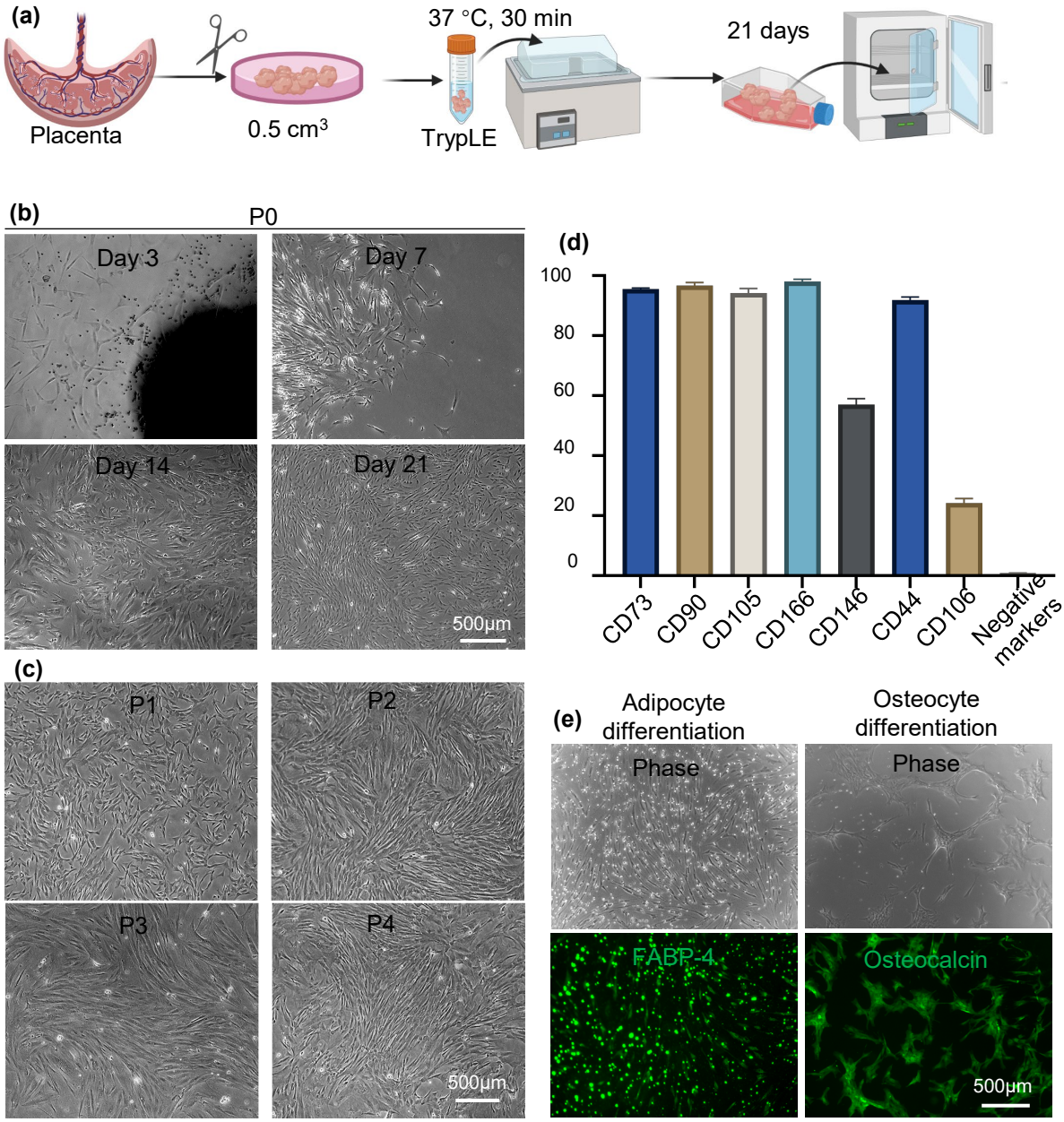

Figure 1. Mesenchymal stromal cell (MSC) isolation and characterization. **(a)** Illustration of the isolation process. **(b)** MSCs migrating out from the tissue. **(c)** MSCs during the expansion phase (Passage 1 to 4). **(d)** Surface marker expression for P4 MSCs. Negative markers include CD34, CD45, CD11b, CD79A, and HLA-DR. **(e)** P4 MSCs could be differentiated into adipocytes and osteocytes

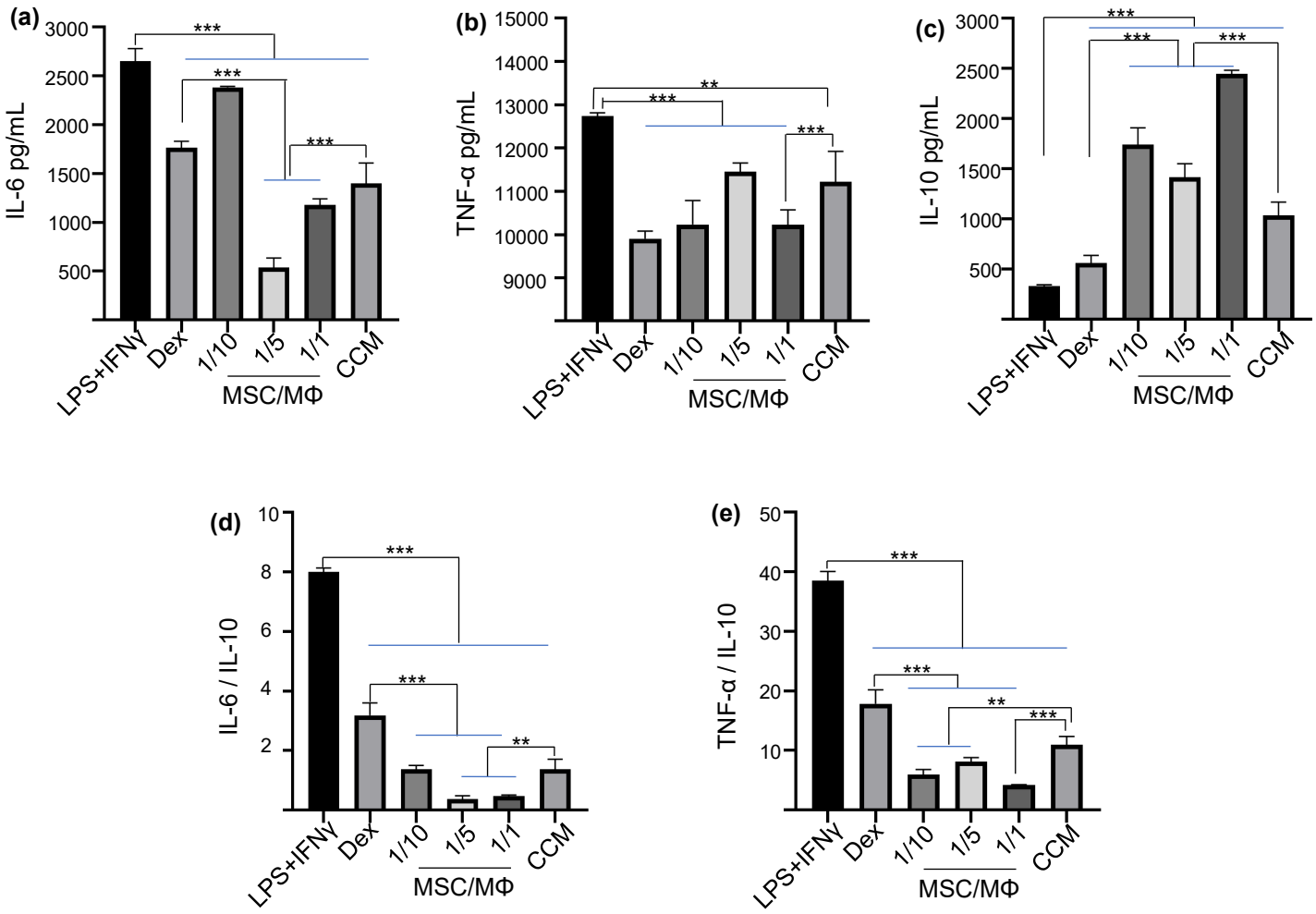

Figure 2. MSCs modulated inflammation in Raw 264.7 macrophages (MΦs). Cells were stimulated with 100 ng/mL LPS and 10 ng/mL IFN-γ and co-cultured with MSCs at different ratios (MSC/MΦ=1/10, or 1/5 or 1/1) or treated with MSC conditioned medium (CCM). Dexamethasone (+Dex, 1 μg/mL) was used to benchmark MSCs' potency. Pro-inflammatory mouse cytokine IL-6 **(a)**, TNF-α **(b)** and anti-inflammatory mouse cytokine IL-10 **(c)** were measured via ELISA. The IL-6/IL-10 **(d)** and TNF-α/IL-10 ratio **(e)** were also shown.

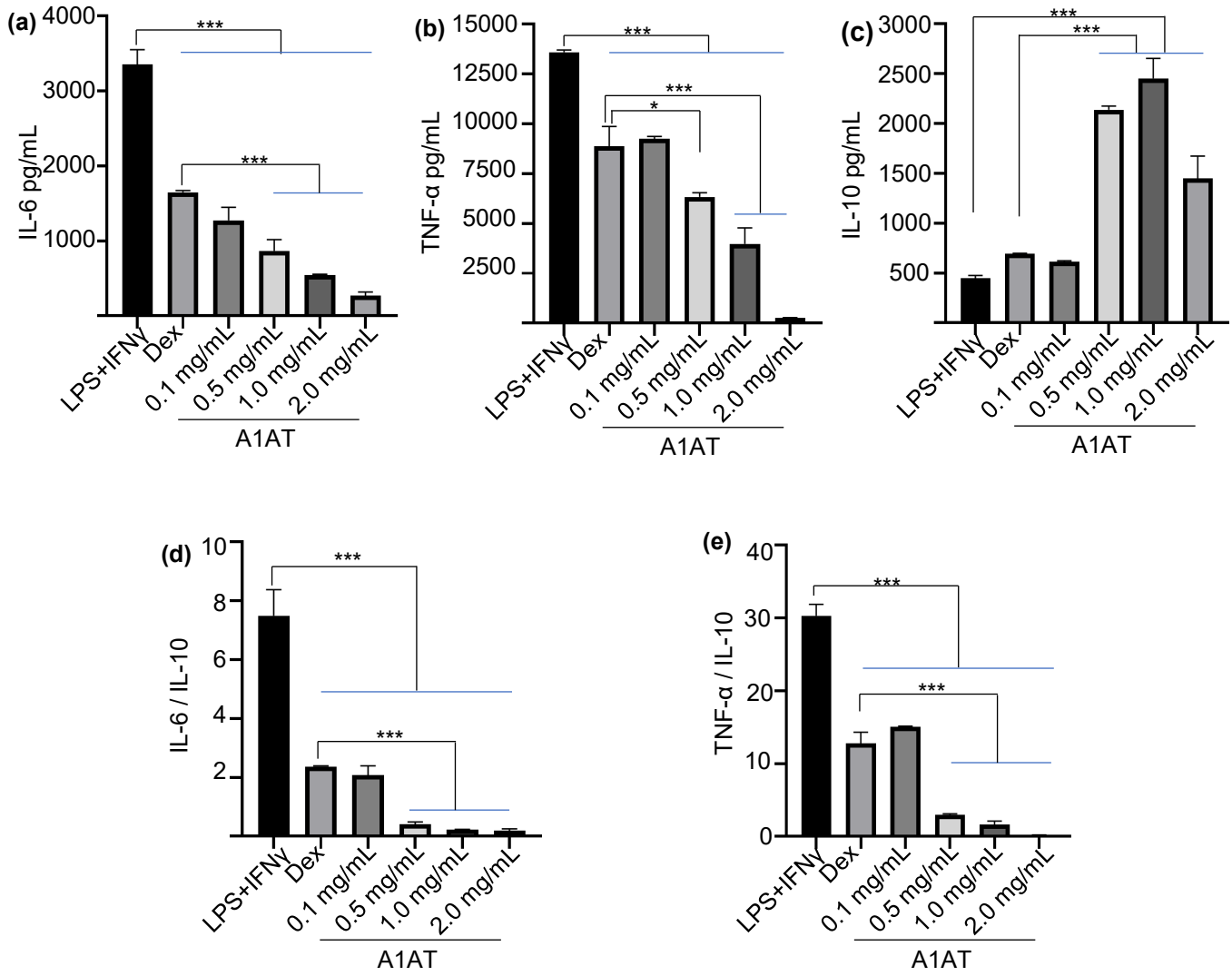

Figure 3. A1AT modulate inflammation in Raw 264.7 MΦs. Cells were stimulated with 100 ng/mL LPS and 10 ng/mL IFN-γ and treated with A1AT at 0.1 to 2 mg/mL. Dexamethasone (+Dex, 1 μg/mL) was used to benchmark MSCs' potency. Pro-inflammatory mouse cytokine IL-6 **(a)**, TNF-α **(b)** and anti-inflammatory mouse cytokine IL-10 **(c)** were measured via ELISA. The IL-6/IL-10 **(d)** and TNF-α/IL-10 ratio **(e)** were also shown.

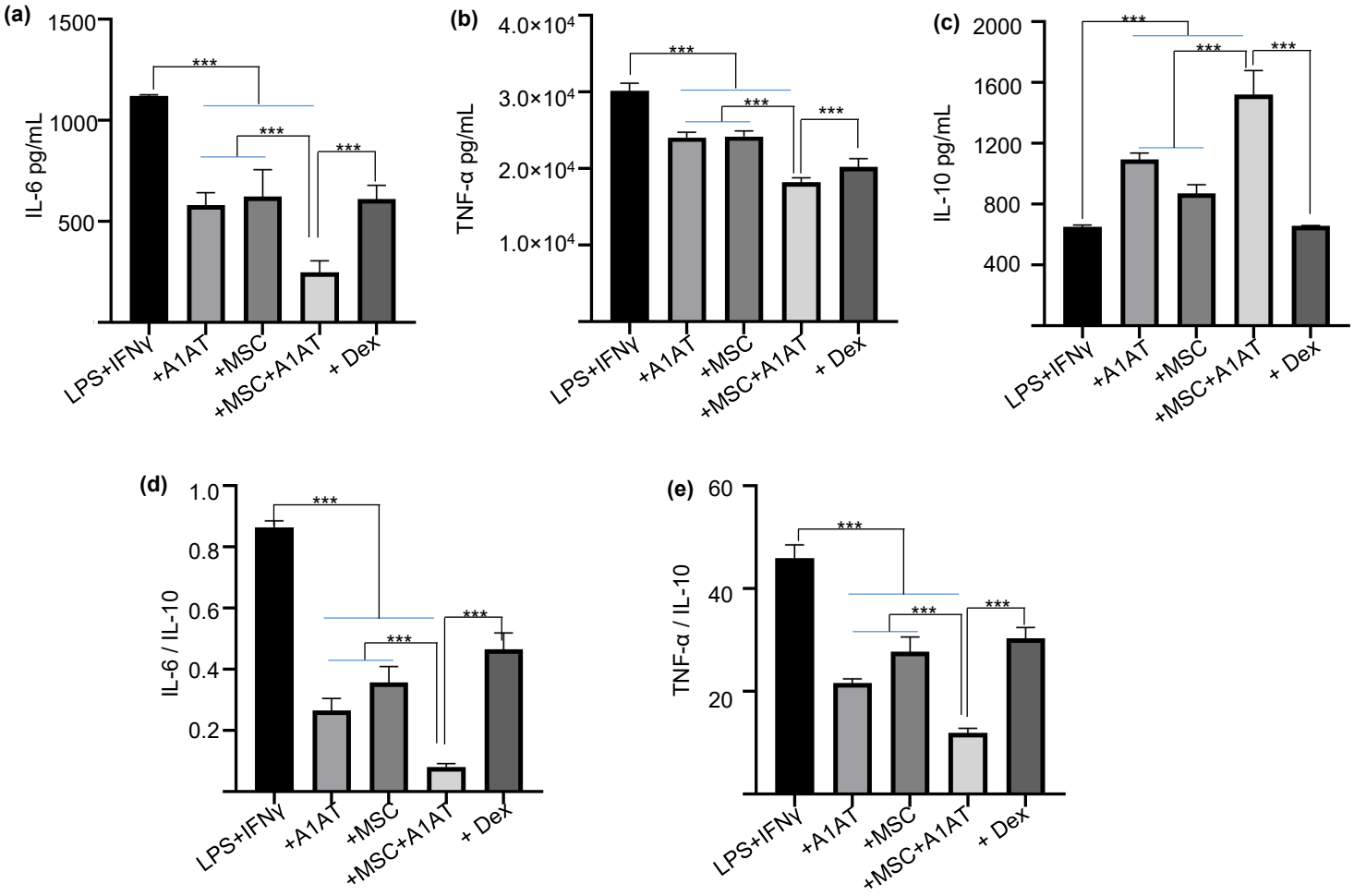

Figure 4. MSC and A1AT had synergy to modulate inflammation in Raw 264.7 MΦs. Cells were stimulated with 100 ng/mL LPS and 10 ng/mL IFNγ and treated with 0.5 mg/mL A1AT or MSCs (MSC/MΦ=1/10) or their combination. Dexamethasone (Dex, 1 μg/mL) was used to benchmark MSCs' potency. Pro-inflammatory mouse cytokine IL-6 **(a)**, TNF-α **(b)** and anti-inflammatory mouse cytokine IL-10 **(c)** were measured via ELISA. The IL-6/IL-10 **(d)** and TNF-α/IL-10 ratio **(e)** were also shown.

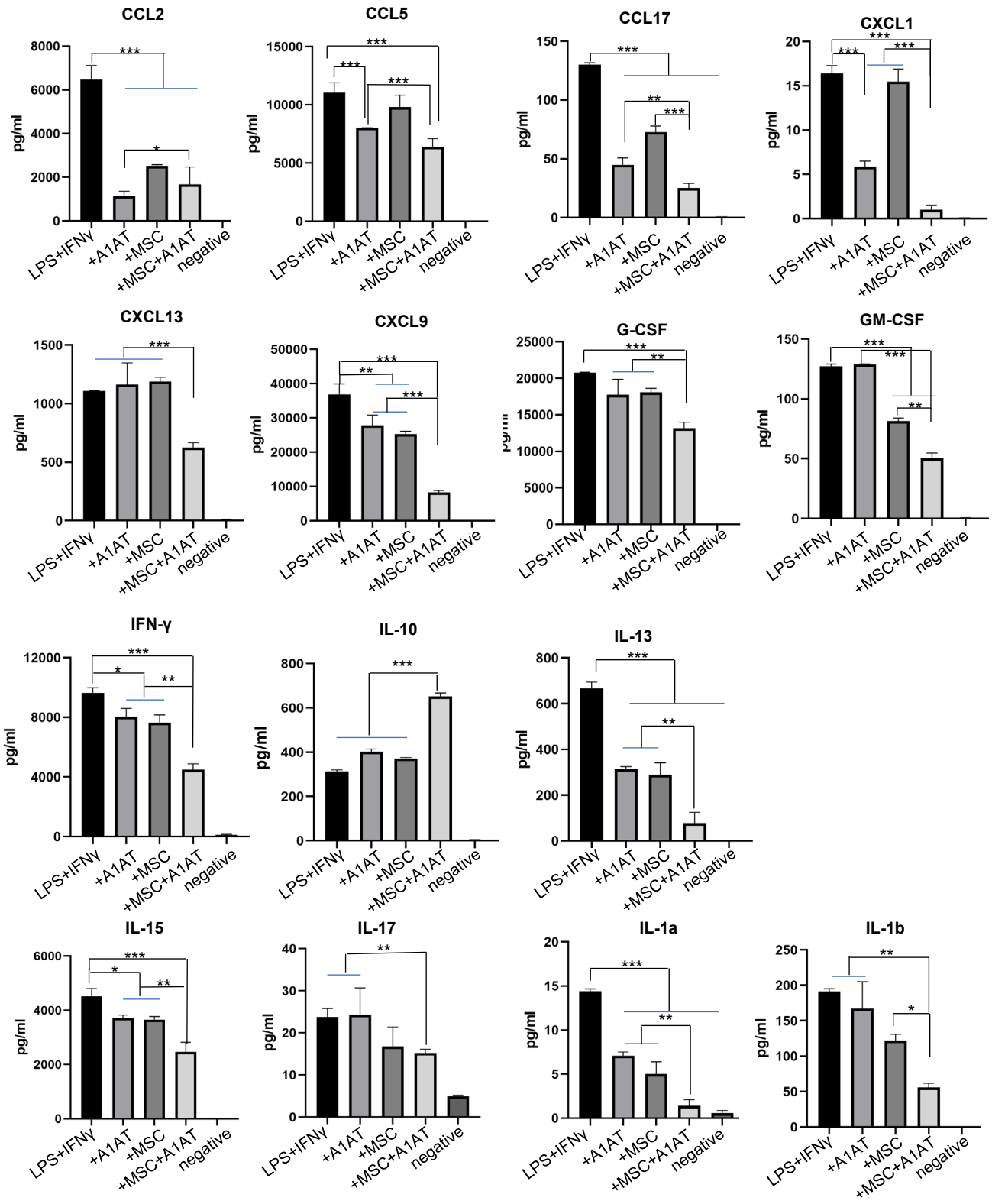

Figure 5. MSC and A1AT had synergy to modulate inflammation in Raw 264.7 MΦs. Cells were stimulated with 100 ng/mL LPS and 10 ng/mL IFNγ and treated with 0.5 mg/mL A1AT or MSCs (MSC/MΦ=1/10) or their combination. Dexamethasone (Dex, 1 μg/mL) was used to benchmark MSCs' potency. 40 mouse cytokines in the medium were measured using antibody array. Negative: cells were not stimulated and had no treatment (more plots in the next page).

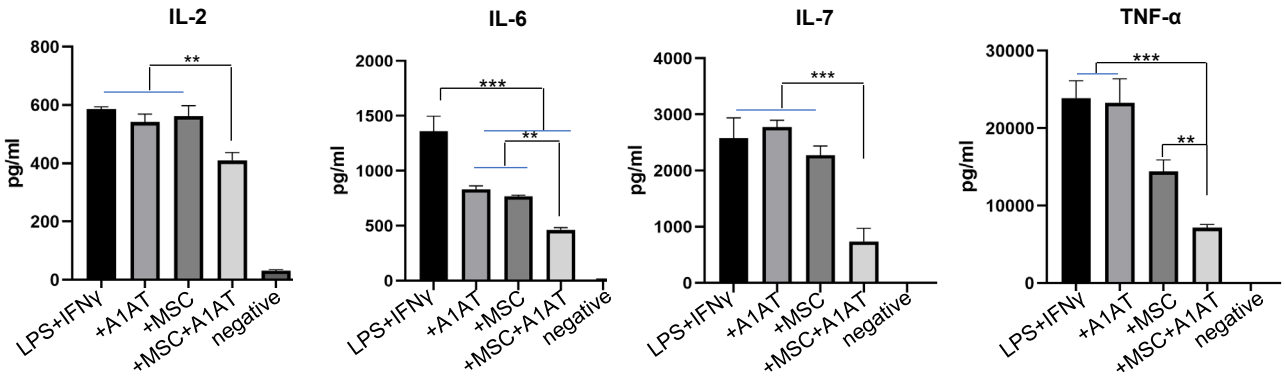

Figure 5. MSC and A1AT had synergy to modulate inflammation in Raw 264.7 MΦs. Cells were stimulated with 100 ng/mL LPS and 10 ng/mL IFNγ and treated with 0.5 mg/mL A1AT or MSCs (MSC/MΦ=1/10) or their combination. Dexamethasone (Dex, 1 μg/mL) was used to benchmark MSCs' potency. 40 mouse cytokines in the medium were measured using antibody array. Negative: cells were not stimulated and had no treatment.

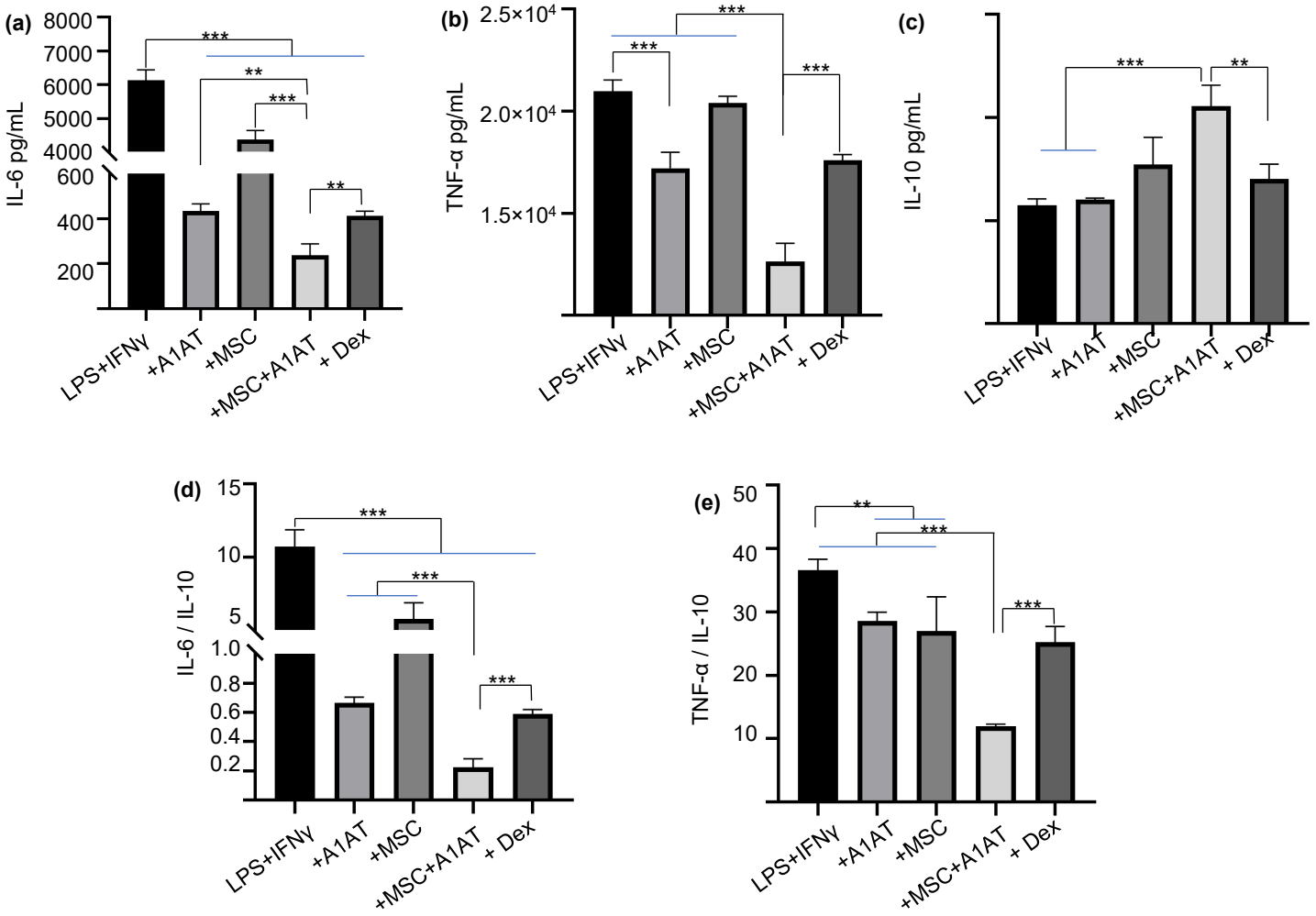

Figure 6. MSC and A1AT had synergy to modulate inflammation in human THP-1 derived macrophages. Cells were stimulated with 100 ng/mL LPS and 10 ng/mL IFNγ and treated with 0.5 mg/mL A1AT or MSC/macrophage = 1/10 or their combination. 1 μg/mL dexamethasone (Dex) was used as control. Proinflammatory human cytokines IL-6 **(a)**, TNF-α **(b)** and anti-inflammatory human cytokine IL-10 **(c)** were measured via ELISA. The IL-6/IL-10 **(d)** and TNF-α/IL-10 ratio **(e)** were also shown.

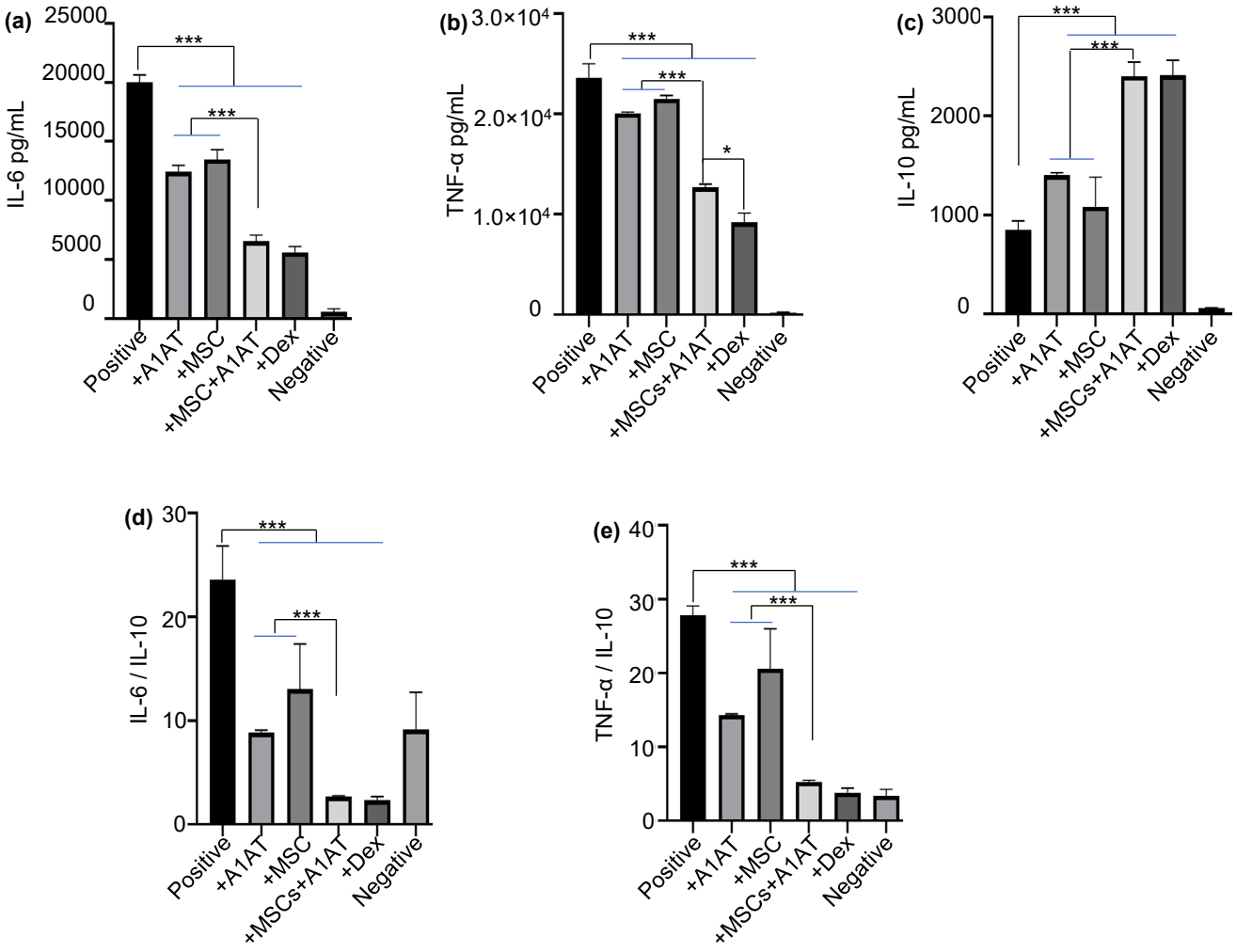

Figure 7. MSC and A1AT had synergy to modulate inflammation in primary human PBMCs. Cells were stimulated with 100 ng/mL LPS + 10 ng/mL IFNγ + anti-CD3/CD28 antibodies (positive control) and treated with 0.5 mg/mL A1AT or MSC/macrophage = 1/10 or their combination. 1 μg/mL dexamethasone (Dex) was used as a benchmark. PBMCs without activation and treatment was used as a negative control. Proinflammatory human cytokines IL-6 **(a)**, TNF-α **(b)** and anti-inflammatory human cytokine IL-10 **(c)** were measured via ELISA. The IL-6/IL-10 **(d)** and TNF-α/IL-10 ratio **(e)** were also shown.

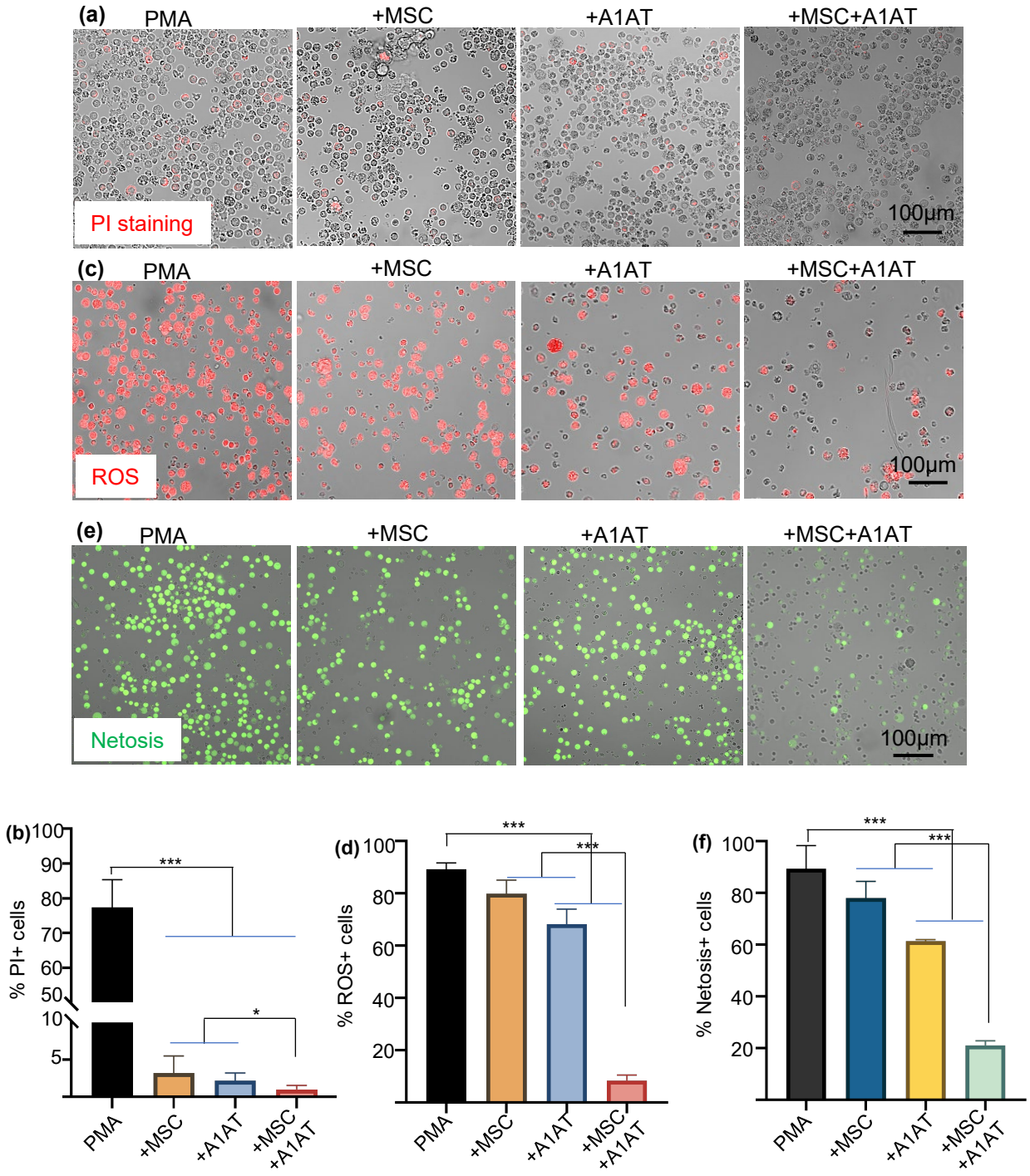

Figure 8. MSC and A1AT combination treatment reduced neutrophil death, ROS burst and NETosis. HL-60 cells derived neutrophils were stimulated with 100 nM PMA and treated with MSC (MSC/Neutrophil = 1/10), 0.5 mg/mL A1AT, or MSC + A1AT for 4 hours. Cell death **(a, b)** ROS burst **(c, d)** and Netosis **(f, g)** analyzed with image flow cytometry.

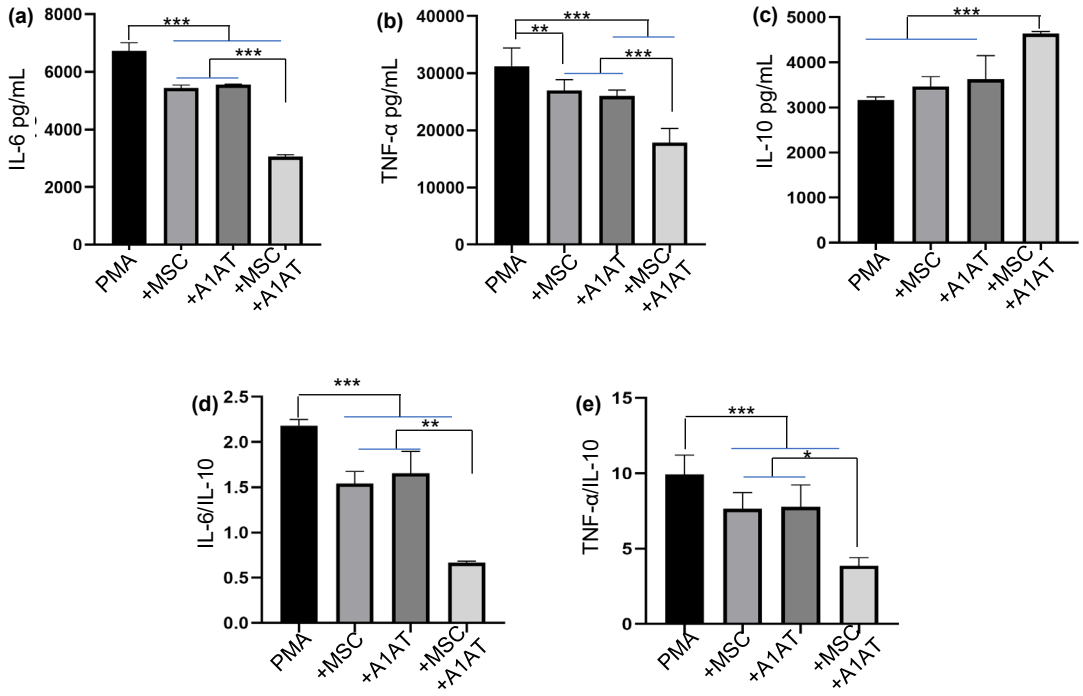

Figure 9. MSC and A1AT combination treatment enhanced the inflammatory modulation in neutrophils. HL-60 cells were differentiated into neutrophils with DMSO (1.25% v/v) and ATRA (0.1 μM) for 3 days. Neutrophils were stimulated with 100 nM PMA and treated with MSC (MSC/Neutrophil = 1/10), 0.5 mg/mL A1AT, or their combination for 4 hours. Pro-inflammatory cytokines IL-6 **(a)**, TNF-α **(b)** and anti-inflammatory cytokine IL-10 **(c)** were measured via ELISA. The IL-6/IL-10 **(d)** and TNF-α/IL-10 ratio **(e)** were also shown.

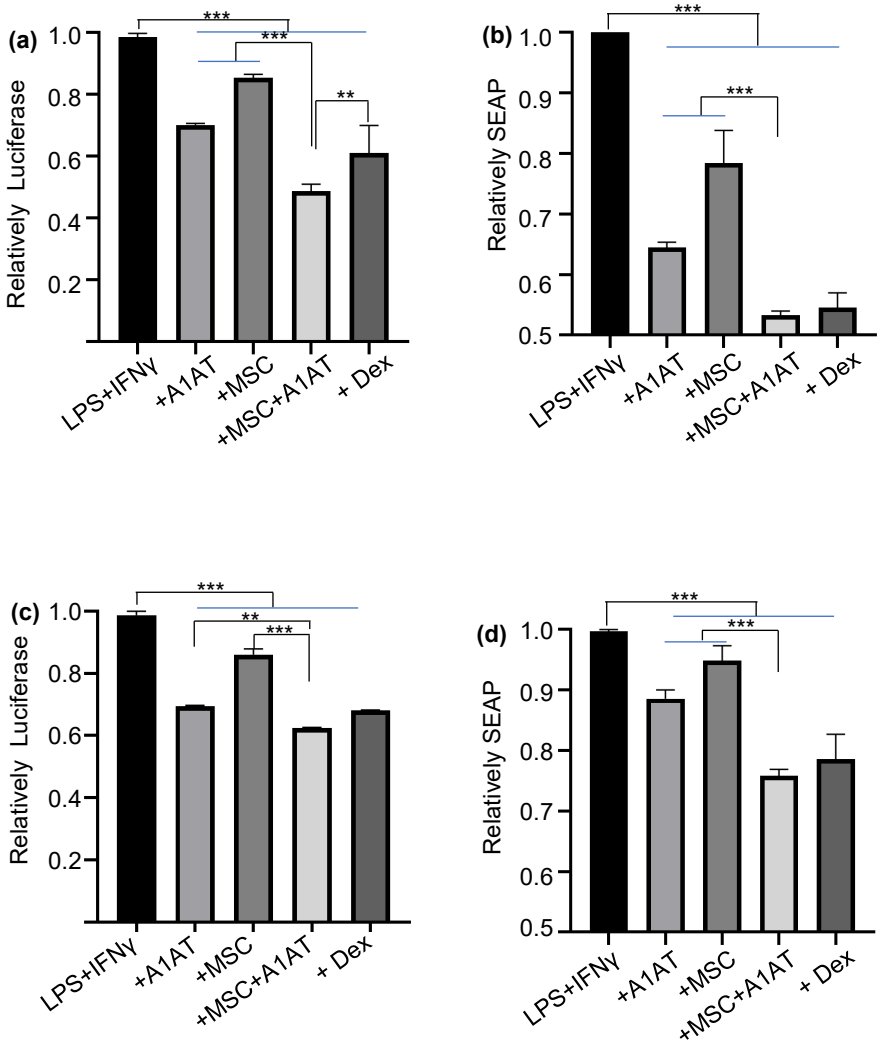

Figure 10. MSC and A1AT had synergy on regulating NF-κB and IRF signaling. Raw 264.7 **(a, b)** and THP1 **(c, d)** cells were engineered to express a luciferase reporter for NF-κB signaling and a secreted alkaline phosphatase (SEAP) reporter for IRF (3 and 9) signaling. THP1 cells were differentiated into macrophages before stimulation. Macrophages were stimulated with 100 ng/mL LPS and 10 ng/mL IFNγ and treated with 0.5 mg/mL A1AT or MSC/macrophage = 1/10 or their combination. 1 μg/mL dexamethasone (Dex) was used as control. Luciferase **(a, c)** and SEAP **(b, d)** activities were quantified.

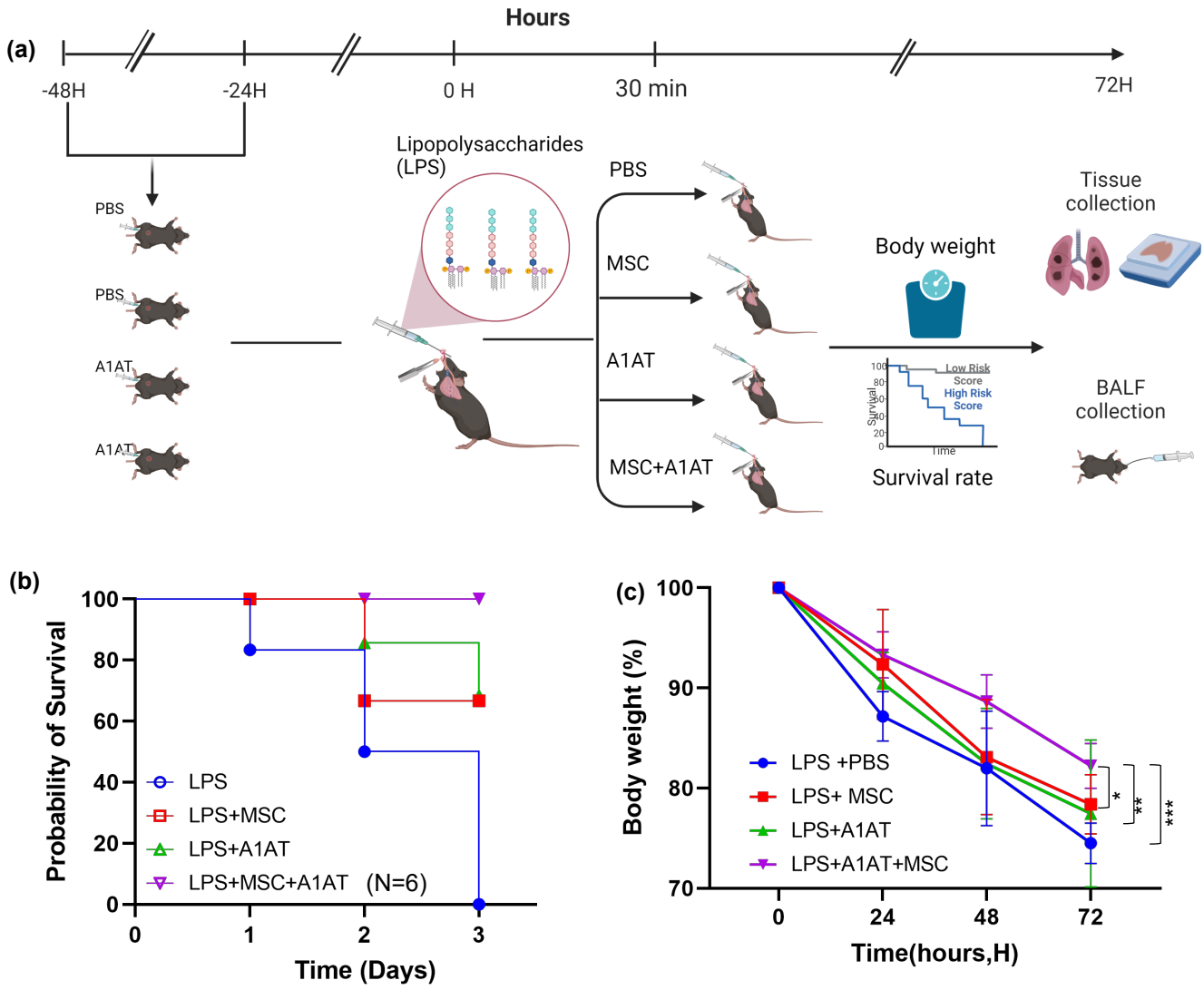

Figure 11. MSC and A1AT showed synergy in increasing survival rate in mice with LPS-induced acute lung injury. **(a)** Illustration of the ALI mouse model. **(b)** The survival rate and **(c)** body weight development.

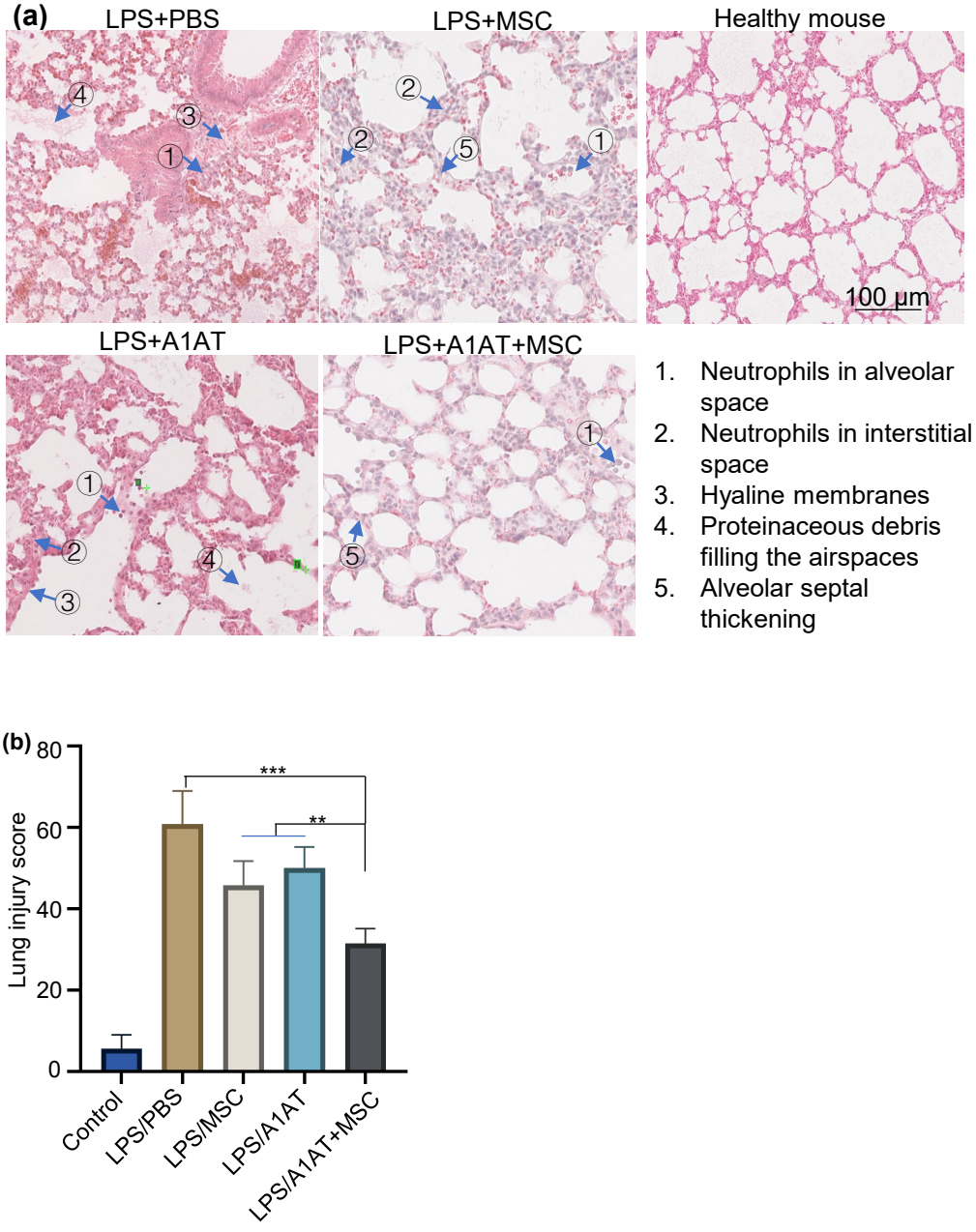

Figure 12. MSC and A1AT showed synergy in reducing lung injury in ALI mice. **(a)** HE staining and **(b)** lung injury scores. The lung injury scores were calculated by the five criteria shown (a).

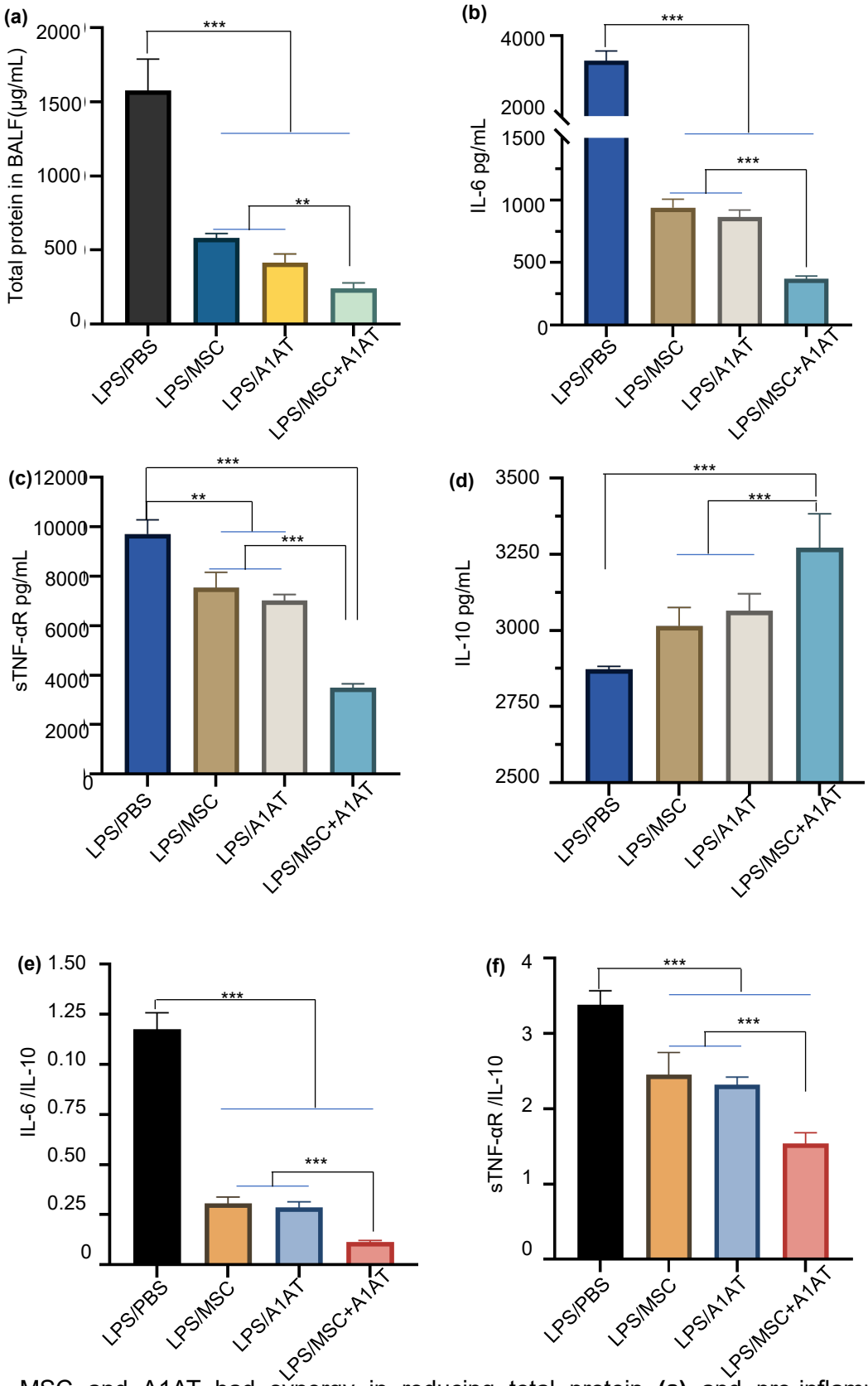

Figure 13. MSC and A1AT had synergy in reducing total protein **(a)** and pro-inflammatory cytokines, while increased anti-inflammatory cytokine IL-10 **(b-f)** in BALF in ALI mouse

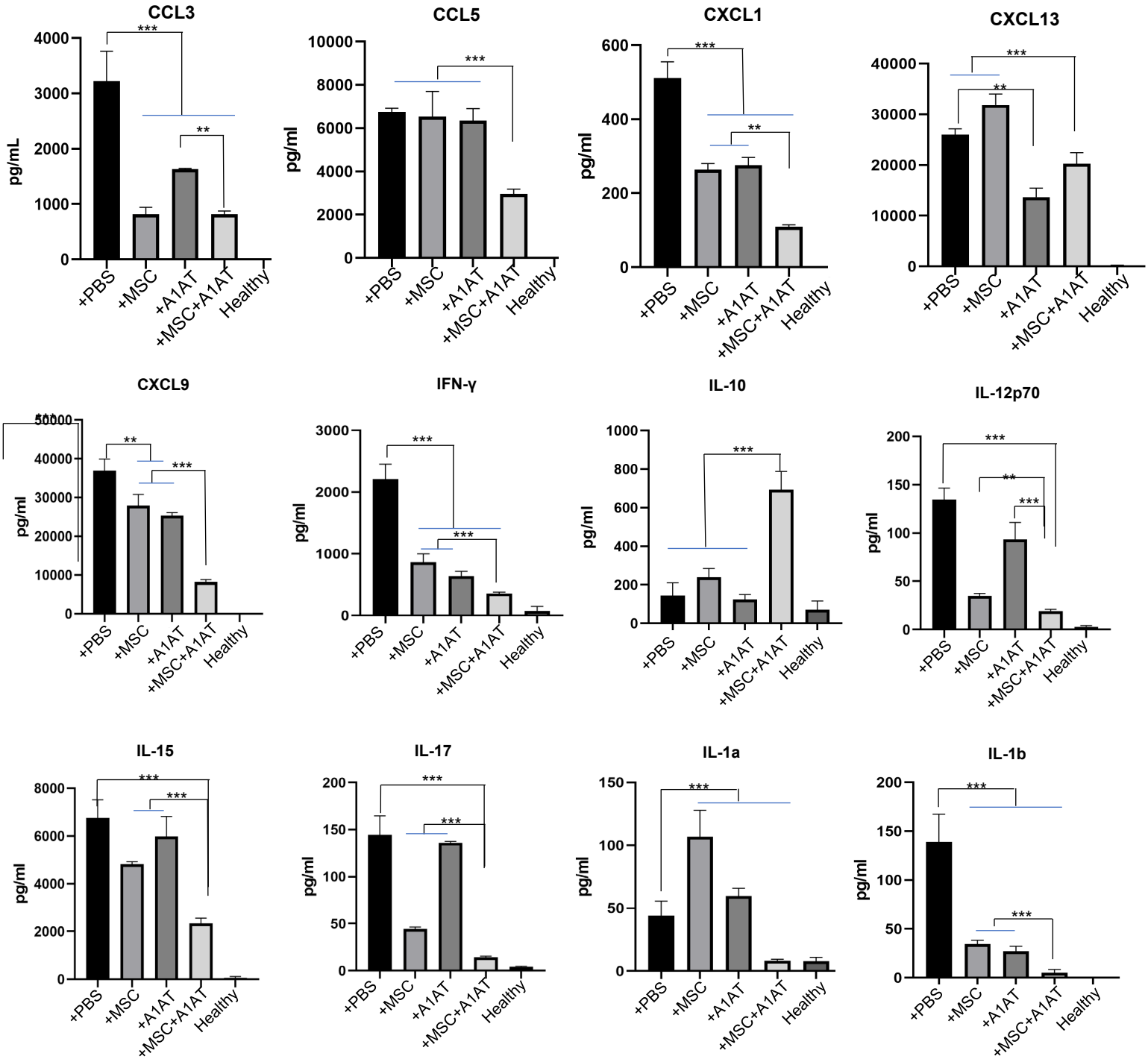

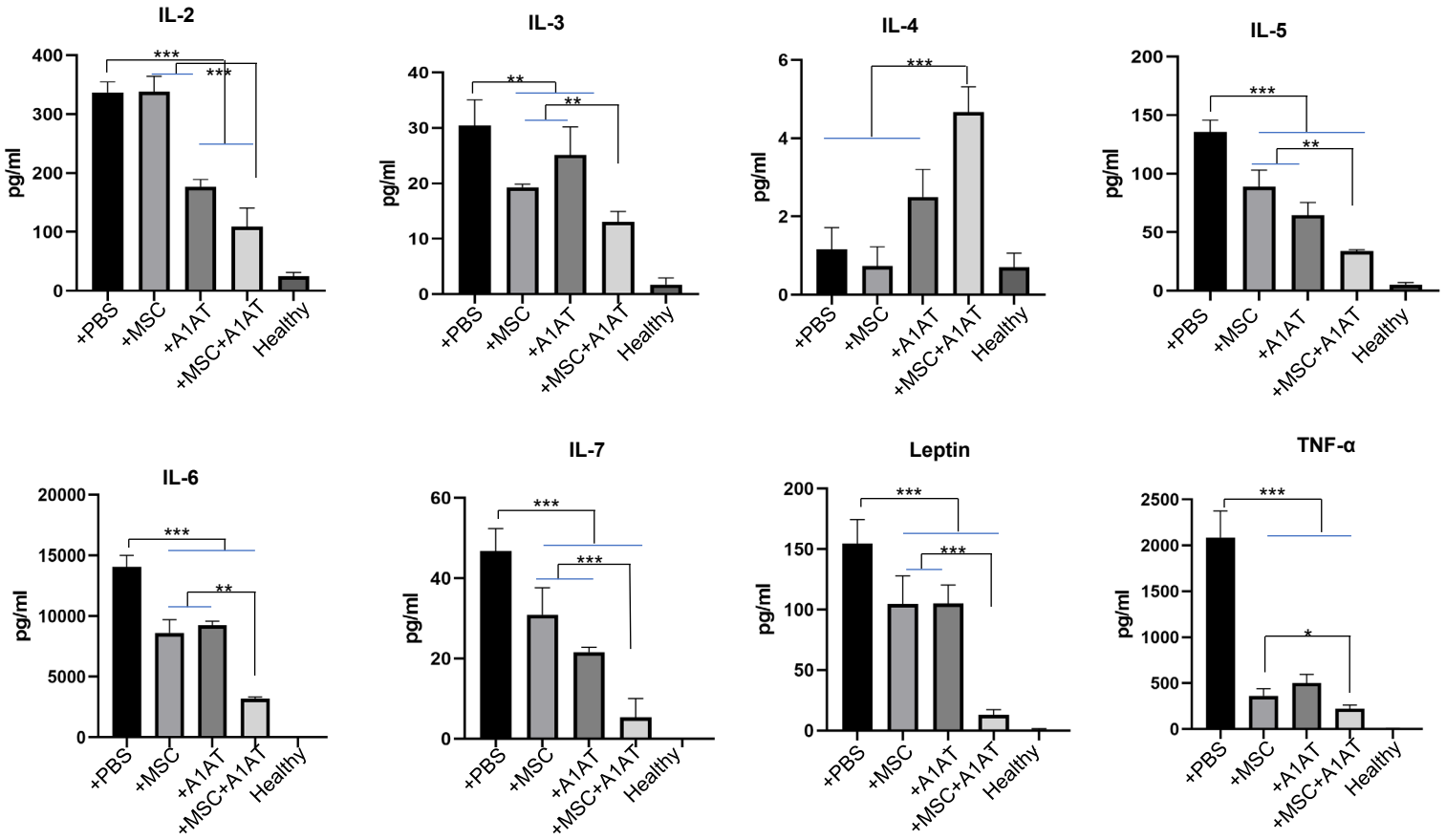

Figure 14. MSC and A1AT combination treatment reduced pro-inflammatory cytokines, while increased anti-inflammatory cytokines in BALF in ALI mouse as measured using Raybiotech inflammation antibody array. Healthy: healthy mouse sample.

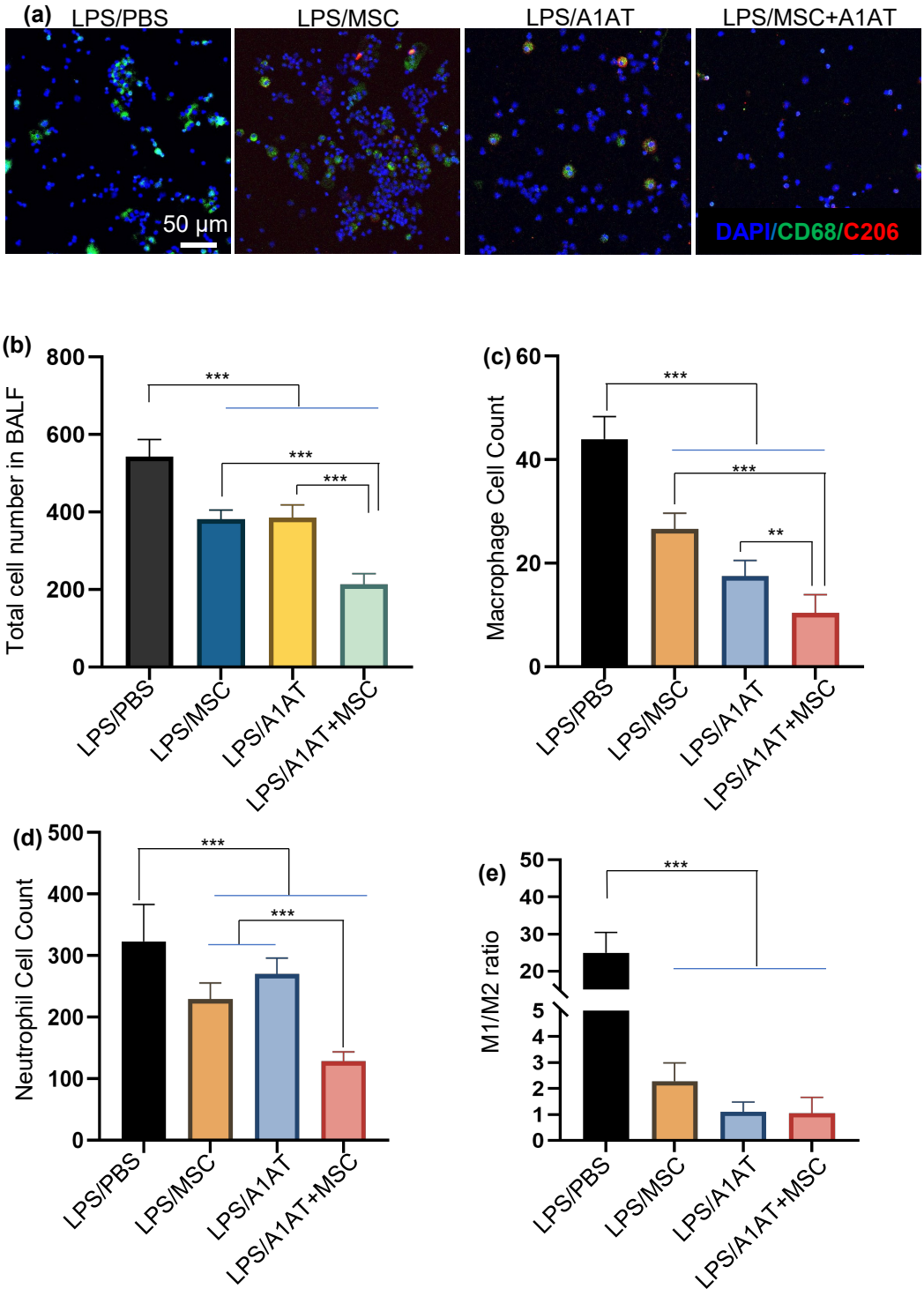

Figure 15. MSC and A1AT combination treatment reduced total the total cell, neutrophil, macrophage numbers in BALF and M1/M2 ratio.

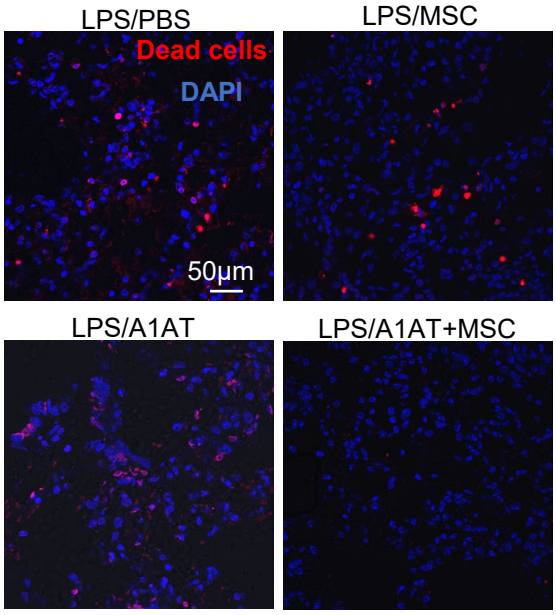

Figure 16. MSC and A1AT had synergy in reducing lung tissue injuries. TUNNEL staining showed the MSCs and A1AT combination treatment group had no dead cells.